Journal
of
The Franklin Institute
Devoted to Science and the Mechanic Arts

Vol. 231 FEBRUARY, 1941 No. 2

THERMODYNAMIC TREATMENT OF THE SWELLING PRESSURE OF COAL.

BY

WALTER FUCHS, Ph.D.,

Professor of Fuel Technology, The Pennsylvania State College.

FUNDAMENTAL CONCEPTS PERTAINING TO THE TOPIC.

(1) During the past few years, numerous investigators have studied the swelling pressure of coal. The published contributions of Mott and Wheeler,[12] Altieri,[1] Brown,[3] Davis and associates,[6] Foxwell,[7] Koppers,[10] and Russell [13] are outstanding; a considerable amount of unpublished experimental work has undoubtedly accumulated. For the past few years this problem has been under investigation at the School of Mineral Industries, The Pennsylvania State College, but as yet no results have been released. Although considerable experimental data are available, no analysis of fundamental concepts has yet been proposed.

The purpose of this discussion is to attempt a theoretical treatment referring to the pressure developed by a coal charge undergoing carbonization. In order to limit this treatment to its fundamental aspects, certain simplifying conditions have been introduced. Such factors as origin, secondary geological changes, differences in rank and type, and details of petrographic and chemical composition may be regarded, for the purpose of this analysis, as immaterial to the basic problem.

(Note—The Franklin Institute is not responsible for the statements and opinions advanced by contributors in the JOURNAL.)

Consideration will first be given to a porous substance which under the influence of increasing temperature passes through one or several fluid stages before decomposing to produce solid and gaseous products. It is fully recognized that most coals decompose to some extent over the entire temperature range, but the introduction of the foregoing restriction offers a useful simplification of the initial mathematical analysis. It will be seen as the analysis develops that this treatment may be made applicable to the general case, in which decomposition may occur over the entire temperature range, by the introduction of the necessary variables into the simplified equations.

(2) Let it be assumed that the substance is charged into an open chamber of rectangular shape; that one of the walls of the chamber is kept at a uniform and constant temperature several hundred degrees above the assumed decomposition point; and that heat is introduced into the charge at a steady rate.

A sequence of qualitative phenomena is easily visualized. After the influx of heat has continued for some time, the layer of substance adjacent to the wall will melt and form a fluid film parallel to the hot wall. As the heat penetrates farther into the charge, substance on the "cool" side of the plastic film is converted into fluid material, while substance on the "hot side" is solidified by a complex chemical reaction. Thus, the plastic layer seems to travel through the charge. But although circulatory movement within the plastic layer will take place it is essentially a state of matter that travels, not matter. Nevertheless, the fictitious movement of a fluid layer through the charge offers a satisfactory starting point to a description of phenomena.

(3) Another result of consideration refers to the temperature of the plastic layer. Let the difference between the temperature of beginning decomposition and the temperature of beginning fusion be called the plastic range, let the interface of the plastic layer next to the heated wall be designated as hot interface and the other one as cold interface, then the following statements are self-evident: The temperature of the hot interface is identical with the temperature of beginning decomposition; the temperature of the cold interface is identi-

cal with the temperature of beginning fusion; the temperature gradient within the plastic layer is equal to the temperature difference within the plastic film, i.e., the "plastic range" divided by the thickness of the plastic layer.

(4) In a general way, the charge undergoing carbonization may be considered as a heterogeneous system, consisting of at least three phases, the coke phase, the plastic layer, and the coal phase. The fluid phase (the plastic layer) is located between the two solid phases. The solid interface is stiff in case of the coke phase, more or less yielding in case of the coal phase. The expanding fluid phase meets two obstacles: the solid interfaces and its own limits of temperature stability. The latter condition checks expansion of the fluid phase into void space: obviously, unless the temperature of the void is within the plastic range, the fluid entering voids (in the charge or above the charge) will either decompose or "freeze," and in both cases the plastic layer is confined to a definite volume.

(5) The following notation will be used in the quantitative treatment:

M = mass, g.
Q = heat, cal.
F = force, dynes.
W = work, ergs, or cm.^{3} at.
E = energy content, cal.
S = entropy, cal.
H = latent heat, cal. g.$^{-1}$
C = heat capacity, cal. g.$^{-1}$ ° C.$^{-1}$
T = temperature, ° K.
t = time, sec.
p = pressure, at.
v = volume, cm.^{3}
A = area, cm.^{2}
L = thickness of plastic layer, cm.
ρ = density, g. cm.$^{-3}$
α = volume expansivity, ° C.$^{-1}$
β = compressibility, at.$^{-1}$
m = mass, l = thickness of the plastic zones of melting and decomposition.

Subscripts s, fl, and g refer to the solid, liquid, and gaseous state, respectively.

Subscripts F and D refer to fusion and decomposition.
Subscript b refers to the bulk density of a solid charge, i.e., its weight per unit space.

APPLICATION OF THE FIRST LAW OF THERMODYNAMICS.

(6) As soon as the cold substance is charged into the chamber described sub (2), heat is transmitted into the charge through a cross-section comprised of solid elements and voids. Temperature and energy content of the charge rise. An element of unit mass, volume v, density ρ and heat capacity C absorbs heat by radiation, convection, and conduction. The following steps are noted:

(*a*) Temperature rise to beginning fusion.
(*b*) Isothermal fusion.
(*c*) Temperature rise to beginning decomposition.
(*d*) Decomposition.

In each step, the relationship between absorbed heat and work is given by the general equation of the first law (1)

$$dQ = dE + dW, \qquad (1)$$

where dW equals $p\,d\,v$. Some results obtained by the application of equation (1) to steps (*a*) to (*d*) are listed:

(*a*) In view of the very small coefficient of expansion of solids, and of the porosity of the charge, the expansion work against atmospheric pressure is negligible.

(*b*) The latent heat of fusion is small, because of the amorphous nature of coal. Unless the charge is very densely packed, and (or) expands upon melting to an unusual extent, fusion results in contraction, i.e., work is absorbed by the element, not expended on the surroundings.

(*c*) Heating of the plastic mass is accompanied by liquid expansion or, if the expansion is hindered, by development of pressure. This is in agreement with practical experience: pressure during carbonization has only been noted with coals known to pass through a plastic stage.

(*d*) Decomposition gives rise to solid and gaseous products. The remarks sub (*a*) apply likewise to the solid expansion of

porous coke. As known by experience, coke occupies usually the same space in the oven as the coal charge: intermediary semicoke might conceivably require more space. Simultaneous shrinking on the cold side and expanding on the hot side will tend to push the fluid towards the coal charge. If the gas formed upon decomposition is allowed to escape, it will perform work against the atmosphere, but not against the oven wall. It is indeed not the high volatile coals, but the low volatile coals that exhibit the greatest swelling pressure.

(7) In order to obtain an estimate of the heat absorbed by the plastic layer, it seems helpful to consider the heat absorbed by a liquid body of rectangular shape, mass M, volume v, density ρ, heat capacity C, one face of the body being kept at a temperature T_1, and the opposite at a lower temperature T. Let the nature of the temperature drop through the liquid body be unknown. If T_1 is equal to $T + \Delta T$, then the equation (2) gives the maximum amount of heat that may be gained by the body.

$$M \int_{T}^{T+\Delta T} dQ = MC\Delta T = MC(T_1 - T). \qquad (2)$$

If Q equals $C.\ (T_1 - T)$, it denotes the maximum amount of heat per gram liquid that may be gained from the heat source; or the maximum amount of heat per gram liquid that will be lost to the surroundings if the temperature of the liquid body drops to the original value T. In case of a finite value $(T_1 - T)$, equation (2) denotes the upper limit of Q. A great number of actual conditions are conceivable, and the actual temperature gradient must be taken into account. If sufficient time has elapsed to reach a stationary state, i.e., after the heat transients have disappeared, then the temperature gradient across the body will become a constant as may be seen from the Fourier heat conduction equation. In this case, the average heat content per gram of the liquid body between the limits will be given by equation (3).

$$Q_{fl} = 0.5\ Q. \qquad (3)$$

If sufficient time has not elapsed to reach a stationary

state, then equation (3) should be replaced by the more general equation (4)

$$Q_{fl} = kQ, \tag{4}$$

where k depends on the actual temperature gradient.

If it is desired to obtain numerical values of heat absorbed in the plastic range, it is necessary to know the corresponding specific heats. Although direct observations are lacking, an estimate can be based upon published work on thermal properties of petroleum products (5,9) and other suitable information, such as referring to the specific heat of coal at ordinary temperatures (8), and to specific heats of glasses (11). An average value of about 0.6 for c_p was derived. Another important quantity for use in calculations is the ratio C_p/C_v. It was concluded from the aforementioned data that, in the range of 380 to 450° C., this ratio does not exceed a value of 1.05–1.06: i.e., in this range C_p and C_v are only about 5 per cent. apart.

(8) Even without an exact knowledge of the heat content of the plastic layer, the pressure due to liquid expansion may be estimated. It is recalled that expansivity α, compressibility β, and coefficient of pressure γ are defined by the differential equations (5).

$$\alpha = \frac{\partial v}{\partial T}\Big)_p; \qquad \beta = -\frac{\partial v}{\partial p}\Big)_T; \qquad \gamma = \frac{\partial p}{\partial T}\Big)_v. \tag{5}$$

From equation (6), equation (7) for the coefficient of pressure is easily derived.

$$dp = \frac{\partial p}{\partial T}\Big)_v dT + \frac{\partial p}{\partial v}\Big)_T dv, \tag{6}$$

$$\frac{\partial p}{\partial T}\Big)_T = -\frac{\partial p}{\partial v}\Big)_T \frac{\partial v}{\partial T}\Big)_p = \frac{\alpha}{\beta}. \tag{7}$$

Expansivity and compressibility of coal in the plastic state have not yet been measured. Preliminary estimates may be based on the assumption that plastic coals are similar in properties to the petroleum products, asphalts and fluxes, studied by Cragoe [5] and Jessup.[9] For α, a value of 0.0004 was obtained. As regards β, the work of Jessup points to an average

coefficient of compressibility of various petroleum products of 0.00036 at 300° C. For the range 375–450° C., a value of 0.0008 may be deduced from the trend of his data at lower temperatures.

These values, $\alpha = 0.0004$ and $\beta = 0.0008$, were later subjected to a more exacting analysis: estimation of α was found to have a higher degree of probability then estimation of β, because of errors inherent to extrapolation of non-linear curves with steep slopes. In view of the fact that the difference $C_p - C_v$ appeared to be established with the same degree of probability than α, equation (13) was used for computation of β. A value of 0.0008 was obtained, in complete accord with the first estimate.

By the use of these values, γ is found to equal 0.5 at. This means that an increase of pressure of 0.5 atmosphere is required to keep the volume of the fluid under consideration constant when heated 1° C.

APPLICATION OF THE SECOND LAW OF THERMODYNAMICS.

(9) Let a liquid body of heat content $M.Q_{fl}$ function as working substance in a cyclic process between the temperature limits T and T_1. This would be accomplished if a fraction m/M of the liquid were steadily withdrawn at either temperature, and put back into the process at the other; e.g., by means of a suitable pump. By selection of the proper pumping speed, the amount of liquid in the process, its particular temperature gradient, and the sum of its kinetic and potential energy, could be kept virtually constant. If both ΔT and the pumping speed are infinitesimal, equation (2) describes adequately the maximum amount of heat available in the cyle. If $(T_1 - T)$ is finite, and the speed of cycling low, equation (3) is to be used. For non-linear temperature gradients, a value for k in equation (4) must be determined.

An attempt is now made at estimating, by the application of the second law of thermodynamics, the maximum work to be obtained if the plastic layer is conceived as a working substance in a cyclic process. Let it be recalled that every perfect engine reversibly working between the same temperature limits has the same efficiency, whatever working substance is

used. The efficiency of a process operated between T_D and T_F equals the ratio of work obtained in the cycle to heat absorbed at the higher temperature, as shown by the equation for maximum work:

$$W = Q_{fl} \frac{T_D - T_F}{T_D}. \tag{8}$$

(10) If extraneous work is excluded, the heat available for transformation under the second law is converted into potential energy: a force is set up within the plastic layer. Equation (9) is an integrated expression of theoretical maximum force: it is based upon consideration of the definition of force, and of equations (2), (3), (4), and (8).

$$FL = 41.31 \frac{T_D - T_F}{T_D} kC(T_D - T_F)AL\rho_{fl}. \tag{9}$$

The figure 41.31 is the factor for transformation of calories into cm.^{3} at. Important conclusions concerning the dependence of the maximum swelling pressure on the plastic range, the temperature of decomposition, the specific heat, the volume and the density of the plastic mass can be drawn at once from equation (9).

EQUATIONS FOR THEORETICAL AND ACTUAL SWELLING PRESSURE.

(11) As stated before, heat absorbed by a plastic layer is converted into energy and work in accordance with the first law of thermodynamics:

$$dQ = dE + dW. \tag{1}$$

If the volume is kept constant, extraneous work is excluded: dW becomes zero, dQ equals $C_v dT$, and equation (10) is descriptive of the relation between pressure and temperature under these conditions:

$$dE = dQ)_v = C_v dT = \frac{\partial Q}{\partial T}\Big)_p dT + \frac{\partial Q}{\partial p}\Big)_T dp. \tag{10}$$

$\frac{\partial Q}{\partial T}\Big)_p$ is, by definition, the specific heat at constant pressure

c_p. For $\left(\frac{\partial Q}{\partial p}\right)_T$ equation (11) was obtained by the use of the Bridgman Tables.[2]

$$\left(\frac{\partial Q}{\partial p}\right)_T = -\left(\frac{\partial v}{\partial T}\right)_p T = -\alpha T. \tag{11}$$

By proper substitution, equation (10) is transformed into equation (12):

$$\alpha T dp = (C_p - C_v)dT. \tag{12}$$

By the introduction of the thermodynamic relation (13)

$$C_p - C_v = \frac{T\alpha^2}{\beta}, \tag{13}$$

equation (12) assumes the simple shape of equation (14):

$$dp = \frac{\alpha}{\beta} dT. \tag{14}$$

By integration of dp between the atmospheric pressure and the theoretical maximum pressure, and of dT between the temperatures of fusion, T_F, and decomposition, T_D, equation (15) is obtained:

$$\int_1^p dp = \frac{\alpha}{\beta} \int_{T_F}^{T_D} dT. \tag{15}$$

Hence, under stated conditions, the theoretical maximum swelling pressure is equal to the ratio of expansivity and compressibility of the plastic layer times the plastic range (16):

$$p = \frac{\alpha}{\beta} (T_D - T_F). \tag{16}$$

In other words, when coal is fused at atmospheric pressure, and not allowed to expand beyond the volume of the fused mass, the pressure to be expected on heating up to the temperature of decomposition is found from equation (16).

By due consideration of equations (3) and (4), equation (16) is transformed into equation (17):

$$p = \frac{\alpha}{\beta} k(T_D - T_F). \tag{17}$$

Equation (17) is the expression for the theoretical maximum pressure developed within a plastic layer travelling with constant minimum volume and low speed through the charge.

(12) In section (11) constancy of volume of the plastic layer has been assumed: for a more general treatment, the volume must be taken as a variable, and the possibility of extraneous work must be admitted. Equation (18), obtained by the combination of the first and second law, holds in all such cases:

$$TdS = dE + dW + \Delta. \tag{18}$$

Δ equals zero in case of reversible change; in the case under consideration its value appears insignificant compared to TdS. It is, therefore, neglected in the following argument. If the state of the system is determined by two variables (x and y), T, S, E, and W may be conceived as functions of x and y (19):

$$T\frac{\partial S}{\partial x}\Big)_y dx + T\frac{\partial S}{\partial y}\Big)_x dy = \left[\frac{\partial E}{\partial x}\Big)_y + \frac{\partial W}{\partial x}\Big)_y\right]dx + \left[\frac{\partial E}{\partial y}\Big)_x + \frac{\partial W}{\partial y}\Big)_x\right]dy. \tag{19}$$

From equation (19), equations (20) and (21) are easily derived:

$$T\frac{\partial S}{\partial x}\Big)_y = \frac{\partial E}{\partial x}\Big)_y + \frac{\partial W}{\partial x}\Big)_y, \tag{20}$$

$$T\frac{\partial S}{\partial y}\Big)_y = \frac{\partial E}{\partial y}\Big)_x + \frac{\partial W}{\partial y}\Big)_x. \tag{21}$$

By differentiation of (20) with respect to y, and of (21) with respect to x, equations (22) and (23) are obtained:

$$\frac{\partial T}{dy}\Big)_x\frac{\partial S}{\partial x}\Big)_y + T\frac{d^2S}{dxdy} = \frac{d^2E}{dxdy} + \frac{d}{dy}\left(\frac{\partial W}{\partial x}\Big)_y, \tag{22}$$

$$\frac{\partial T}{\partial x}\Big)_y\frac{\partial S}{\partial y}\Big)_x + T\frac{d^2S}{dxdy} = \frac{d^2E}{dxdy} + \frac{d}{dx}\left(\frac{\partial W}{\partial y}\Big)_x. \tag{23}$$

By subtraction of (23) from (22), equation (24) results:

$$\frac{\partial T}{\partial y}\Big)_x\frac{\partial S}{\partial x}\Big)_y - \frac{\partial T}{\partial x}\Big)_y\frac{\partial S}{\partial y}\Big)_x = \frac{d}{dy}\left(\frac{\partial W}{\partial x}\Big)_y - \frac{d}{dx}\left(\frac{\partial W}{\partial y}\Big)_x. \tag{24}$$

As far as the writer is aware, equation (24) has first been developed and fully discussed by Clausius.[4] Some values for the expression on the right hand side of equation (24) are given in Table I.

TABLE I.

Relationship between "Work-difference" and Choice of Variables.

x.	y.	Work-difference.
v	p	1
v	T	$\frac{\partial p}{\partial T}\Big)_v$
p	T	$-\frac{\partial v}{\partial T}\Big)_p$

Volume and pressure are now selected as variables for the further treatment of equation (24):

$$\frac{\partial T}{\partial p}\Big)_v \frac{\partial S}{\partial v}\Big)_p - \frac{\partial T}{\partial v}\Big)_p \frac{\partial S}{\partial p}\Big)_v = 1. \tag{25}$$

For the derivatives of entropy, values as given in equations (26) and (27) are substituted:

$$\frac{\partial S}{\partial v}\Big)_p = -\frac{\partial S}{\partial p}\Big)_v \frac{\partial p}{\partial v}\Big)_S, \tag{26}$$

$$\frac{\partial S}{\partial p}\Big)_v = -\frac{\partial v}{\partial T}\Big)_S. \tag{27}$$

In textbooks of thermodynamics, equation (27) is usually listed as a "Maxwell relation." It is readily obtained from the Clausius equation (24) by selection of p and T as variables, and by the use of Table I. Equation (28) finally assumes the simple shape of equation (31).

$$\frac{\partial T}{\partial p}\Big)_v \frac{\partial v}{\partial T}\Big)_S \frac{\partial p}{\partial v}\Big)_S + \frac{\partial T}{\partial v}\Big)_p \frac{\partial v}{\partial T}\Big)_S = 1, \tag{28}$$

$$\frac{\partial p}{\partial v}\Big)_S + \frac{\partial p}{\partial T}\Big)_v \frac{\partial T}{\partial v}\Big)_p = \frac{\partial p}{\partial T}\Big)_v \frac{\partial T}{\partial v}\Big)_S, \tag{29}*$$

* Isothermal and adiabatic changes are connected by the relationship (29a)

$$\frac{\partial p}{\partial v}\Big)_T = \frac{C_v}{C_p}\frac{\partial p}{\partial v}\Big)_s. \tag{29a}$$

It has been noted that the ratio of the specific heats of plastic coal is probably quite close to unity.

$$dp = \frac{\partial p}{\partial T}\Big)_v dT - \frac{\partial p}{\partial T}\Big)_v \frac{\partial T}{\partial v}\Big)_p dv, \qquad (30)$$

$$dp = \frac{\alpha}{\beta} dT - \frac{1}{\beta} dv. \qquad (31)$$

Upon integration of (31), equations (32) and (33) are obtained:

$$\int_1^p dp = \frac{\alpha}{\beta}\int_{T_F}^{T_D} dT - \frac{1}{\beta}\int_{v_{min.}}^{v_{max.}} dv, \qquad (32)$$

$$p = \frac{\alpha}{\beta}(T_D - T_F) - \frac{1}{\beta}(v_{max.} - v_{min.}). \qquad (33)$$

p is the swelling pressure, i.e., the driving pressure against the atmosphere.

Equation (34) is derived from equation (33) in view of equations (2), (3), and (4):

$$p = \frac{\alpha}{\beta} k(T_D - T_F) - \frac{1}{\beta}(v_{max.} - v_{min.}). \qquad (34)$$

Equation (33) represents a more general formula than is expressed in equation (16). It is readily recognized that equation (17) follows from (34), if $(v_{max.} - v_{min.})$ becomes zero.

Application of equation (34) is illustrated in Table II.

TABLE II.

Corresponding Values of p and v Derived from Equation (34).

$k = 0.5$; $(T_D - T_F) = 25$; $\alpha = 0.0004$; $\beta = 0.0008$

p	6.25	5.00	3.75	2.50	1.25	0	at.
v	1	1.001	1.002	1.003	1.004	1.005	ccm.
confinement	100	80	60	40	20	0	%

Volume and confinement are correlated by equation (35):

$$\% \text{ confinement} = \frac{v_{max.} - v_{act.}}{v_{max.} - v_{min.}} 100. \qquad (35)$$

(13) A maximum swelling pressure develops when the two advancing plastic layers meet and coalesce. After the union

of the two layers, heat can no longer be transferred to substance with a temperature below the temperature of fusion. Consequently, the temperature gradient through the plastic mass changes, and there is a moment at which it may be conceived that practically the entire plastic mass, still present at this moment, has a rather uniform temperature just below the temperature of decomposition. Under these circumstances, an amount of heat dQ introduced into the plastic mass will occasion a change of temperature dT, of pressure dp, and of volume dv. Equation (36) is descriptive of these changes.

$$dp = \frac{\partial p}{\partial T}\Big)_v dT + \frac{\partial p}{\partial v}\Big)_T dv. \tag{36}$$

By proper substitution of the partial derivatives, equation (37) follows immediately from (36):

$$dp = \frac{\alpha}{\beta} dT - \frac{1}{\beta} dv. \tag{37}$$

Equation (37) is identical with equation (31) of this paper. In the integrated equation (38), ΔT stands for the plastic range, and Δv for the actual volume expansion of the plastic mass at its highest temperature; for $\Delta v = 0$, equation (38) gives the theoretical maximum swelling pressure.

$$p = \frac{\alpha}{\beta} \Delta T - \frac{1}{\beta} \Delta v. \tag{38}$$

For the arbitrary case discussed in section (12), Table II, a maximum swelling pressure of 12.5 at. is obtained.

(14) The question may be raised whether the isothermal decomposition of the plastic layer, and the corresponding loss of entropy, has an influence on the swelling pressure. An answer to this question is obtained by an examination of the differential equation (39):

$$dp = \frac{\partial p}{\partial S}\Big)_{T_D} dS. \tag{39}$$

For the partial derivative shown in equation (39), equation

(40) is obtained by the introduction of p and T as variables into equation (24):

$$\frac{\partial p}{\partial S}\Big)_{T_D} = -\frac{\partial T}{\partial v}\Big)_{p} = -\frac{1}{\alpha'}. \tag{40}$$

Equation (40) indicates the pressure change due to the entropy change brought about by decomposition of the plastic mass. Inspection reveals that this equation is actually identical with the Clausius-Clapeyron equation for isothermal changes of state; hence, α' refers to the difference of the specific volumes of gaseous and liquid plastic mass. Then, in equation (41), ΔH is defined as the latent heat of the contemplated change:

$$\int_0^{\pi} dp = -\frac{1}{\alpha'}\int_{S_1}^{S_2} dS = -\frac{1}{\alpha'}\frac{\Delta H}{T_D}. \tag{41}$$

A rough estimate of the expression on the right hand side of equation (41) is presented. Let it be assumed that the vaporized plastic mass occupies from 100 to 1000 times more space than the liquid plastic mass, and that the latent heat of vaporization may be any amount from 10 to 1000 calories. Then, all possible values of the expression are in the range from 0.01 to 0.00001 calory, i.e., entirely negligible.

DISCUSSION OF VARIOUS CONDITIONS OF RESTRAINT.

(15) In the preceding discussion, two restricting conditions have been maintained, namely, (a) no heat producing or consuming processes occur within the plastic layer, and (b) the plastic layer consists of only one phase. These restrictions are now examined.

(a) The heat produced (or consumed) by a chemical process within the plastic layer must be added to (or deducted from) its heat content. The numerical value of the heat integral will change because of a changed temperature gradient within the plastic layer. It should be emphasized, however, that the heat content of the plastic layer cannot exceed the value given by equation (2).

(b) Equation (34) may be regarded as a summary of the discussion of an essentially homogeneous (or monophasic)

plastic layer. In this section, attention is turned to polyphasic plastic layers. Four possibilities are selected as topics of a brief discussion:

1. *Liquid-Solid Systems.*—Surface-active solids will slightly modify the heat content of the plastic layer through heats of adsorption. Inert solids will consume some heat by friction; an additional possibility is mentioned in the discussion of liquid-solid-gaseous systems.

2. *Liquid-Liquid Systems.*—The plastic layer may be comprised of more than one liquid phase, i.e., in case of incomplete miscibility: a minimum pressure is conceivable for a region of complete miscibility, and critical phenomena are possible.

3. *Liquid-Gaseous Systems.*—The condition of coexistence of plastic phase and gas phase is equality of pressure in both phases. If the swelling pressure exceeds the gas pressure, the gas bubbles will be compressed until equality of pressure is restored. If the gas pressure exceeds the swelling pressure, the gas phase will expand until equal pressure again prevails throughout the system, or else, until the plastic layer is "blown up" to a foam. Such excessive gas evolution will have the same effect as maximum expansion. Insufficient provision for the escape of this gas may occasion considerable pressure against the wall; this pressure, however, will be gas pressure, not swelling pressure.*

4. *Liquid-Solid-Gaseous Systems.*—The solid particles may function as "boiling stones" thus facilitating escape of gas.

REMARKS CONCERNING THE INFLUENCE OF TIME AND THE THEORY OF MEASURING DEVICES.

(16) From practical experience, the pressure is known to vary with time. The change of pressure with time is explained by phenomena concomitant with the travelling of the plastic layer. A readily expanding, readily flowing plastic layer will readily surround and dissolve the coal particles in its way: no rise of pressure will be noted until the end of the coking. On the other hand, if the plastic layer is not of the

* The amount of gas present in the plastic layer of various coals and blends is being investigated.—Viscosity, often considered as an important factor, is closely related to thermal expansion and compressibility.[9]

readily expanding and flowing type, increasing confinement is conceivably caused by the pushing of coal particles towards the center of the oven as the plastic layer advances, and a resulting increase of bulk density with time.

In order to obtain a description of the change of pressure with time, equation (34) is differentiated as shown in equation (42)

$$\frac{dp}{dt} = \frac{\alpha}{\beta}\Delta T\frac{dk}{dt} - \frac{1}{\beta}\frac{d(\Delta v)}{dt}. \tag{42}$$

If k is essentially constant, and the amount of confinement remains unchanged, no change of pressure is possible while the plastic layer advances. If k remains constant, while the amount of confinement increases with time, equation (42) is transformed into equation (43):

$$\frac{dp}{dt} = \frac{1}{\beta}\frac{d(\Delta v)}{dt}. \tag{43}$$

In view of the interdependence of swelling pressure and bulk density, equation (43) may also be written:

$$\frac{dp}{dt} = \frac{d\rho_b}{dt}\frac{dp}{d\rho_b}, \tag{44}$$

where ρ_b designates the bulk density of the charge.

(17) If α, β, T_D and T_F are known, the theoretical maximum pressure can be obtained from equation (16) or (33). The relationship between actual and maximum pressure can be expressed in a formal way, either by equation (45):

$$p_{\text{actual}} = p_{\text{max.}} f(p_{\text{max.}}) \tag{45}$$

or by equation (46) which can be derived from equation (33):

$$p_{\text{actual}} = p_{\text{max.}} - \frac{1}{\beta}\Delta v. \tag{46}$$

Equation (46) is descriptive of a straight line with intercept $p_{\text{max.}}$ and slope $-\frac{1}{\beta}$. At present, no satisfactory method is known of ascertaining the expansion of the plastic layer Δv as defined by equation (33). However, equation (46) can be

used within limitations if it is assumed that extrusion of coke beyond a standard reference volume is roughly proportionate to work done by the expanding plastic layer and hence, in a measure, to Δv. By plotting, in a series of observations, observed maximum pressures against amounts of extrusion, the theoretically predicted trend was confirmed: other conditions being equal, high swelling pressures coincided with low extrusion values, and vice versa. Of course, the maximum pressure at zero extrusion is largely determined by the experimental conditions, and is not identical with the theoretical maximum pressure of the thermodynamic formulas.

SUMMARY.

Formulas for the swelling pressure of coal during carbonization have been derived from the first and second law of thermodynamics. Estimates have been used for various otherwise unavailable thermodynamic properties. Application of formulas has been illustrated by means of suitable examples.

ACKNOWLEDGEMENT.

Acknowledgement is made to Professors T. C. Benton, V. Conrad, H. A. Everett, K. deJuhasz, and P. H. Schweitzer of The Pennsylvania State College for valuable help and constructive suggestions.

REFERENCES.

1. ALTIERI, *Proc. Am. Gas Assoc.* (1935), pp. 812–836.
2. BRIDGMAN, "A Condensed Collection of Thermodynamic Formulas," Harvard University Press (1925).
3. BROWN, *Proc. Am. Gas Assoc.* (1938), pp. 640–679.
4. CLAUSIUS, "Abhandlungen über die Mechanische Wärmetheorie," Zweite Abteilung, pp. 45–48, Braunschweig (1867).
5. CRAGOE, U. S. Dept. of Commerce, Bur. of Standards, Misc. Publ. 97 (1933).
6. DAVIS, ET AL, U. S. Bur. of Mines Report of Investigations 3451 (1939).
7. FOXWELL, *J. Inst. Fuel*, 12, 281 (1939).
8. FUCHS, "Die Chemie der Kohle," p. 280, Berlin (1931).
9. JESSUP, Nat. Bur. Standards, *J. of Research*, 5, 985 (1930).
10. KOPPERS, "The New Koppers Expansion Apparatus," Koppers Co., Essen (1936).
11. MOREY, "The Properties of Glass," New York (1938).
12. MOTT AND WHEELER, "Coke for Blast Furnaces," London (1930).
13. RUSSELL, Am. Inst. Min. Met. Eng., *Techn. Publication*, 1118 (1939).

Scales for Evaluating Components of Magnetic Attraction.—A set of scales has been developed by the Geophysical Section of the Geological Survey, United States Department of the Interior, by means of which magnetic anomalies due to geologic bodies of any size or shape on any known or assumed distribution of magnetization may be evaluated. While these scales were originally constructed for evaluating magnetic anomalies, they are equally useful for solving problems involving all fields under the inverse square law, such as gravitational attraction, electric fields, intensity of illumination, etc. A set of 39 scales, drawn on a scale modulus of one inch equals one unit, on two sheets suitable for mounting, has been photolithographed from a master set prepared by the Section of Geophysics. The set contains one scale for each multiple of $\frac{1}{2}$ unit from one to twenty units inclusive. The scale values are computed for a point source of pole strength of 1000 magnetic units. They may be obtained from the Director, Geological Survey, Washington, D. C.

R. H. O.

How Should Engineers Describe a Surface?—In discussing this subject in *Mechanical Engineering*, Vol. 62, No. 10, O. R. SCHURIG concludes that the geometrical characteristics of a surface profile are so numerous that the shape of a surface cannot be adequately described by a single parameter of its profile. The following geometrical characteristics have been suggested or considered in connection with the description of a surface: maximum height from highest to lowest point; average height above base line passing through lowest point; form factor, being the ratio of average height to maximum height above base line; root-mean-square average height with respect to center line of profile; prevailing wave length; direction of irregularities above or below the prevailing surface contour; direction of finish marks with respect to coördinates of the surface; available contact area of unit nominal area. Efforts should be concentrated to determine what geometrical qualities are important for surfaces used in different kinds of applications and in different industries. Once the significant qualities have been agreed on they should be used as a basis for standards covering the description and designation of surface quality. The standards should provide adequately for describing waviness, roughness, and surface flaws.

R. H. O.

I. ON A NEW METHOD OF MEASURING THE MEAN HEIGHT OF THE OZONE IN THE ATMOSPHERE

BY

JOHN STRONG,

California Institute of Technology.

INTRODUCTION.

The amount of ozone overhead in the stratosphere varies from about 1 to 4 mm. when represented as a layer of pure gas reduced to normal temperature and pressure. Ozone present in such a small amount, compared with the other atmospheric gases (see Table I), would not seem to be an important constituent. On the contrary, it is very important in astrophysics, meteorology, geophysics and biology because of its absorption of ultraviolet light to produce the short wavelength limit for the spectrum of the sun and other astronomical bodies at $\sim$ 3000 A. In a paper on atmospheric ozone, Ladenburg [1] writes, "Without the presence of ozone in the stratosphere, life on earth would not exist in its present form. The ultraviolet radiation from the sun exerts strong physiological effects upon every organism, as for example formation of erythems, destruction of bacteria, production of vitamins. The very shortest wavelengths of the sun have the greatest effect on the human skin. Small changes of the intensity of the sun in this region of the spectrum are biologically very (significant). These facts account for the wide interest and the general importance of the study of the atmospheric ozone."

The absorption which makes the atmosphere entirely opaque at wavelengths less than 2913 Å is due to the Hartley ozone band. Partial absorption by this Hartley band extends to the Huggins bands which occupy the spectral region from 3200 to 3300 Å. There is also significant ozone absorption in the visible spectrum by the Chappius bands.

The Hartley and Huggins bands have been employed by

[1] R. W. Ladenburg, *J. O. S. A.*, **25**, 259 (1935).

TABLE I.

Composition of the Atmosphere in the Troposphere and Approximate Reduced Thickness of Separate Constituents at N.T.P.

(Authority for per cent. by volume: F. A. Paneth, *Quarterly Journal of the Royal Meteorological Society*, 63, 433 (1937)).

Constituent.	Per cent. by Volume.	Reduced Thickness.
Nitrogen	78.09	6200 Meters
Oxygen	20.95	1560 "
Argon	0.93	79.5 "
Water	——	10–100 "
Carbon dioxide	0.03	2.4 "
Neon	1.8×10^{-3}	15.1 Centimeters
Helium	5.3×10^{-4}	4.2 "
Krypton	1×10^{-4}	7.9 Millimeters
Hydrogen	5×10^{-5}	4.0 "
Xenon	8×10^{-6}	0.6 "
Ozone	1×10^{-6}	1–4 "
Radon	6×10^{-18}	——

Ozone constituent is variable in amount. The value 1×10^{-6} per cent. applies to country air near the surface of the ground. 1–4 mm is the integrated ozone thickness for the whole atmosphere.

many investigators to study atmospheric ozone. These investigators have used as sources direct sunlight, zenith skylight, starlight and terrestrial sources such as the hydrogen continuum.[2]

The most significant ozone absorption in the infrared is produced by the strong oscillation-rotation band of the mole-

[2] The investigations of atmospheric ozone are treated and bibliographies are to be found in the following review articles:

C. Fabry and H. Buisson, "Mémorial des Sciences Physiques de l'Acad. des Sci. de Paris," Vol. XI, 1930.

F. W. Paul Götz, "Ergebnisse d. kosm. Physik," Vol. I, 1931; Vol. III, p. 253, 1938.

G. B. M. Dobson and A. R. Meetham, "Some Problems of Modern Meteorology," Chapter 15, Published by the Royal Meteorological Society; London 1934.

R. W. Ladenburg, *J. O. S. A.*, **25**, 259 (1935).

"Conference on Atmospheric Ozone held at Oxford, September 9 to 11, 1936," Published by the Royal Meteorological Society; London, 1936.

Rudolf Penndorf, "Beiträge zum Ozonproblem," *Veröffentlichungen der Geophysikalischen Instituts der Universität Leipzig*, **8**, No. 4, 1936.

C. L. Pekeris, *Bulletin of the American Meteorological Society*, **20**, 3 (1939).

W. W. Coblentz and R. Stair, *J. Research N. B. S.*, **22**, 573 (1939).

cule at 9.6 μ. This band falls in a spectral region where the atmosphere is otherwise relatively transparent. This band was discovered by K. Ångstrom [3] and it has been studied by him as well as by others in the laboratory and in the earth's atmosphere.[4]

All these investigations have built up a considerable fund of information about atmospheric ozone correlating it with meteorological, astronomical and geographical factors.

It has been determined that the ozone concentration in the atmosphere is about 1×10^{-6} per cent. by volume at the surface, and this concentration increases with height and reaches a maximum concentration at about 22 k.m. The total amount of ozone in the atmosphere is about twenty times more than that which one would expect from the surface concentrations, assuming uniform distribution. The major part of the ozone of the atmosphere is between the surface and a height of 35 k.m. The variations in the amount of ozone occur mainly between the heights 10 and 20 k.m.

The total amount of ozone fluctuates from day to day and it has been definitely determined that these fluctuations are associated with meteorological factors: relatively large amounts of ozone are associated with cyclonic depressions, relatively low amounts of ozone with anticyclonic pressure highs; also, abnormally high amounts of ozone are associated with polar air masses, low ozone with tropical air masses.

A primary result of the studies of the amount of ozone overhead is that there is no apparent regular night and day variation in the amount. There are, however, fluctuations throughout the day—and indeed, these fluctuations are sometimes so pronounced that the terms "ozone holes" and "clouds of ozone" have been suggested to describe them.

---

[3] K. Ångstrom, *Arch. f. Math., Astron. och. Phys.*, 1, 345 and 395 (1904).

[4] E. Ladenburg and E. Lehmann, *Ann. d. Physik*, 21, 305 (1906).
Eva von Bahr, *Ann. d. Physik*, 29, 780 (1909).
F. E. Fowle, *Smithsonian Misc. Coll.*, 68, No. 8, p. 41 (1917).
J. Devaux, *C. R.*, 193, 1207 (1931); 198, 1595 (1934); 201, 1500 (1935).
Arthur Adel, V. M. Slipher and E. F. Barker, *Phys. Rev.*, 47, 580 (1935).
Arthur Adel and C. O. Lampland, *Astrophys. J.*, 91, 481 (1940).
John Strong, *Phys. Rev.*, 55, 1114 (1939).
John Strong and Kenichi Watanabe, *Phys. Rev.*, 57, 1049 (1940).

There is a very definite annular variation of the amount of ozone overhead. It exhibits a maximum in the local spring of the hemisphere and a minimum in the local fall.

Measurements taken at various stations over the surface of the earth show that the ozone content of the atmosphere increases from the equator to the poles.

Measurements of the vertical distribution of the ozone are not very consistent, but they agree in showing that ozone is a stratified gas, the only one in the atmosphere, and further, they agree in showing that the maximum ozone concentration exists at a height of about 22 k.m. The inconsistency of the results of various observations is perhaps to be expected and explained as due to fluctuations in vertical distribution produced by differing meteorological, astronomical and geographical factors.

PREVIOUS OZONE HEIGHT MEASUREMENTS.

The mean height of the ozone has previously been determined by three main methods which will be described here briefly.

1. The first method uses direct sunlight. Logarithms of the ratio of intensities at two wave-lengths falling within the Hartley ozone band are determined throughout a morning or afternoon and these logarithms are plotted, as ordinates, against the corresponding secants of the zenith distance of the sun as abscissa. One obtains a set of points of which the ones corresponding to a relatively high sun lie on a straight line (providing, of course, that meteorological conditions are steady throughout the measurements). For values of sec z greater than about 2 the points begin to deviate from this straight line, and these deviations increase rapidly as sec z becomes larger. These deviations are due to the curvature of the earth and to the fact that the ozone exists at an average height, h, which is not negligible in comparison with the radius of the earth ρ. The optical path length of sunlight in the ozone stratum is not proportional to sec z. Rather, it is proportional to sec ζ where ζ is the angle of incidence which the sunbeam makes with the plane of the stratum. Sec ζ may be considered equal to sec z only when the sun is high.

Otherwise, z and ζ are related as follows:

$$\sin \zeta = \frac{\sin z}{1 + \frac{h}{\rho}}. \qquad (1)$$

Sec ζ and sec z are related, so

$$\sec \zeta = \sec z \left[1 - \frac{h}{\rho} (\sec^2 z - 1) \right]. \qquad (2)$$

Eq. 2 is only valid when $\sec^2 z \gg \frac{h}{\rho}$.

The mean height h^* is that one of several values of h, which on trial yields the best straight line when the aforementioned logarithms are plotted against corresponding sec ζ, calculated by means of h^*.

This method of determining the height of the ozone layer was first applied by Cabannes and Dufay [5] and yielded $h^* \sim 45$–50 k.m. This result appears to have been unreliable. More recent observations,[6] employing the same method have since yielded heights of $h^* \sim 22$ k.m. in substantial agreement with the heights obtained by other methods.

Three weaknesses of the method are: firstly, that it is only applicable when meteorological conditions are steady—the method assumes, without *prima facie* justification, that the amount and height of the ozone remain constant throughout the observation period; and secondly, the method requires at least a full half day's observations; and finally, the method is not very accurate—under favorable conditions the error of height being at least $\pm$ 5 k.m.

2. The second method, due to Götz [7] and named the *Umkehr* method, uses zenith skylight rather than direct sunlight. It will facilitate our understanding of this method to consider the relationship, which we would expect to obtain between the distribution of energy in the near ultraviolet

[5] J. Cabannes and J. Dufay, *J. de Physique et le Radium*, **8**, 125 (1927).

[6] F. W. P. Götz, A. R. Meetham and G. M. B. Dobson, *Proc. Roy. Soc.*, **145(A)**, 416 (1934).

[7] F. W. P. Götz, *Gerlands Beitr. Geophys.*, **31**, 119 (1931).

spectrum of the zenith skylight and that of the sun. Assume an ozone free atmosphere and of Rayleigh scattering. Let I_s and I_s'' be the intensities of zenith skylight at 3110 and 3290 Å received at the observing station and let $I_\odot$ and $I_\odot''$ be the intensities of direct sunlight at 3110 and 3290 Å received at the observing station. Neglecting the differential loss of energy from the direct solar beam by scattering, the ratio of skylight to sunlight is

$$\frac{I_s}{I_\odot} = B\lambda_1^4 \quad \text{and} \quad \frac{I_s''}{I_\odot''} = B\lambda_2^4 \tag{3}$$

and, taking ratios and logarithms, we get

$$\log \frac{I_s}{I_s''} = \log \left(\frac{3110}{3290}\right)^4 + \log \frac{I_\odot}{I_\odot''}. \tag{4}$$

Now consider the effect of ozone absorption: we have already noted that if observed values of $\log I_\odot/I_\odot''$ are plotted as ordinate against $\sec z$, as abscissa, a set of points is obtained, for a relatively high sun, which lie on a straight line. It is observed, as we would expect from Eq. 4, that the effect of ozone absorption on zenith skylight is analogous: again, for a relatively high sun, a plot of $\log I_s/I_s''$ versus $\sec z$ yields points lying on a straight line. Line is parallel to the line obtained for direct sunlight but displaced vertically by an amount $\log (3110/3290)^4$. The significance of this is that the sunlight is scattered by the zenith sky at a level below the ozone stratum—the total amount of ozone penetrated at a given zenith distance of the sun is, for both the skylight and the sunlight, the same. But as the sun lowers, the change in the sky spectrum by ozone absorption no longer simulates the change produced in the direct solar beam.

For convenience, Götz plots $\log I_s''/I_s$ as ordinates against z^4 as abscissa. Just before sunset, the values of $\log I_s''/I_s$ become stationary in respect to z^4 and for greater values of z there is a reversal of the derivative of $\log I_s''/I_s$ and $\log I_s''/I_s$ approaches the values that obtained when the sun was high. See Fig. 1. This reversal is known as the "Umkehreffekt."

A reversal is to be expected: when the sun is sufficiently low ($z > 90°$), the level of scattering of the zenith skylight

for both wave-lengths will occur entirely above the ozone stratum and observed values of $\log I_s''/I_s$ will be approximately the same as those observed for a high sun owing to the fact that the amount of ozone penetrated is the same.

To further explain the reversal qualitatively, we may think of skylight as reflected sunlight and of the sky as being a peculiar "mirror" located at a definite height overhead. This "mirror" has the properties that its total reflectivity may

FIG. 1.

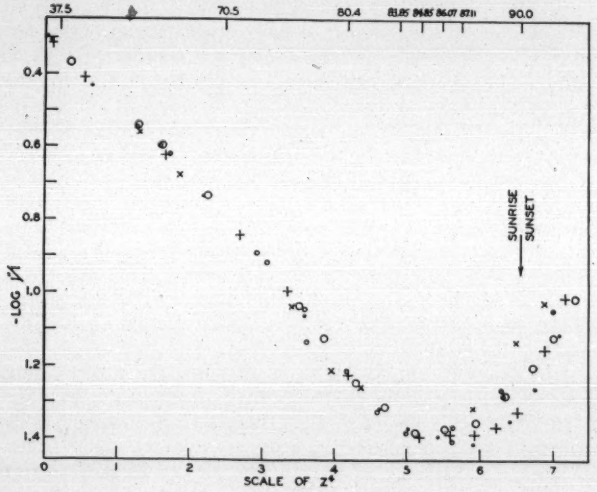

vary as the sun goes lower, but the energy distribution of the "reflected" light (apart from ozone absorption) does not vary. Now when the sun is high, the "mirror" lies below the ozone stratum, but as the sun descends, the "mirror" rises and finally, as the sun goes below the horizon, the "mirror" will go above the ozone stratum. To determine the height and distribution of the ozone it only remains to connect the height of this "mirror" with the height of the sun. A com-

plicated analysis is actually involved in reducing the measured Umkehr curve.[8]

Although an analysis of a composite Umkehr curve, free from casual errors, yields the approximate distribution of ozone in the vertical,[6] an Umkehr curve for a single day, or half-day, allows only the mean height of the ozone to be determined, and this to an accuracy of ± 1.5 k.m.

The Umkehr method requires, as a minimum, a full half day's observations and in effect it determines the height only at a special time near sunset (or sunrise).

3. The third method employs an apparatus which is carried aloft by means of a manned or unmanned balloon. The apparatus continuously measures the ozone overhead as it ascends and these measurements are connected with the height of the balloon by means of a recording barometer, also carried aloft. The method was applied by O'Brien, Mohler and Stewart[9] on the flight of *Explorer II* which occurred on November 11, 1935. The method has also been applied by the Regeners[10] who sent a quartz spectrograph aloft with unmanned balloons. The method has been applied by Coblentz and Stair[11] who used unmanned balloons with a photocell-filter technique for measuring the ozone overhead.

These height measurements are now all in substantial agreement in placing the center of gravity of the ozone at a height of about 22 k.m.

In regard to the vertical distribution the stratosphere flight of *Explorer II* showed very little ozone below a height of 16 k.m. (See Fig. 2.) The Bureau of Standards' work confirms this result in so far as it shows very little ozone below 11 k.m. In contrast with this, the earlier Regener result together with the Umkehr results[6] show considerable ozone in the troposphere. However, the later Regener result shows less ozone in the troposphere than the earlier Regener result or the results from the Umkehr method. The opinion of the

[8] See reference 6. Also, S. Chapman, *Phil. Trans. London*, **234A**, 205 (1935).

[9] Brian O'Brien, Fred L. Mohler and H. S. Stewart, Jr., *National Geographic Soc. Contr. Tech. Papers*, Statosphere Series, No. 2, p. 71 (1936).

[10] Erich and Victor H. Regener, *Physik. Zeits.*, **34**, 788 (1934). Victor H. Regener *Zeits. für Physik.*, **109**, 642 (1938).

[11] W. W. Coblentz and R. Stair, *J. Research N. B. S.*, **22**, 573 (1939).

FIG. 2.

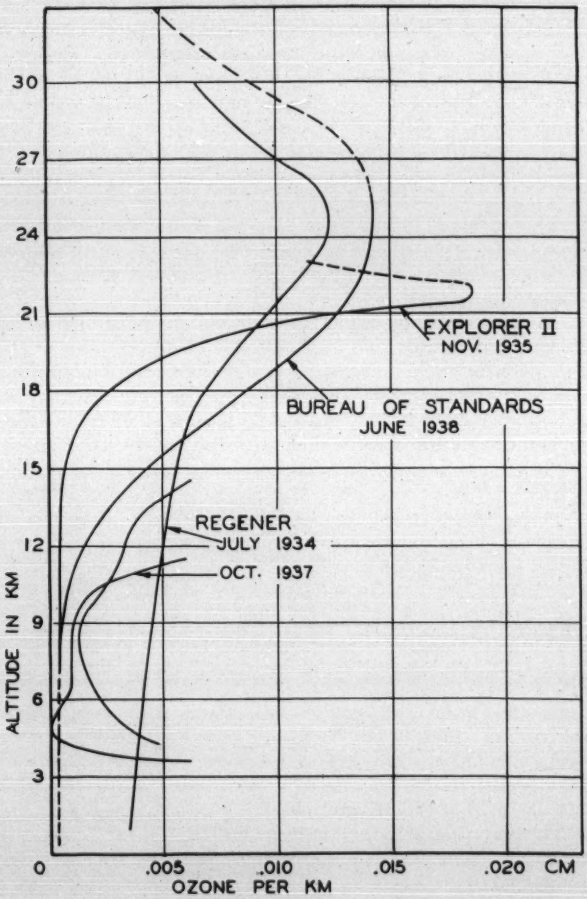
30
27
24
21
18
15
12
9
6
3
0
ALTITUDE IN KM
.005
.010
.015
.020 CM
OZONE PER KM
EXPLORER II
NOV. 1935
BUREAU OF STANDARDS
JUNE 1938
REGENER
JULY 1934
OCT. 1937

author is, with Vassy,[12] that the ozone content of the atmosphere, as regards amount, distribution in the vertical, and temperature, is characteristic of the locale (polar or tropical region) where the obtaining air mass originated. Thus the result of the early flight of the Regeners would appear to be characteristic of a polar type air mass, while the result of the flight of *Explorer II* would appear to be characteristic of a tropical type air mass.

NEW METHOD OF DETERMINING OZONE HEIGHT.

A new method has been developed for measuring the height of the ozone.[13] It is the primary purpose of this paper to describe this new method and to present some of the results obtained.

In general, the new method employs direct sunlight and the height determination may be made at all positions of the sun. Ten to twenty height determinations may be obtained in a day's observations when the weather is clear. This method, in contrast with all the older methods, makes possible the continuous study of the height of the ozone during sunny weather regardless of the steadiness of meteorological conditions.

In particular, the new method measures the intensity of absorption of sunlight by three absorption bands: absorption in the ultraviolet by the Hartley band for the purpose of determining the total amount of ozone overhead; the absorption in the infrared by the Φ-band of water vapor at 1.14 μ in order to find out the total amount of water vapor overhead; and finally, in the infrared, the absorption at 9.6 μ. The solar radiation at this last wave-length is attenuated by both ozone absorption and water vapor absorption. The major part of the atmospheric absorption here is due to the strong π-type oscillation-rotation band of ozone. The remainder of the absorption at 9.6 μ due to water vapor is accounted for with the help of the Φ-band measurement.

The new method functions owing to the fact that the ultraviolet absorption in the Hartley band is substantially

[12] Mme A. Vassy and M. E. Vassy, *La Météorologie*, No. 19, Jan.–Feb. (1939).

[13] John Strong, *Phys. Rev.*, **55**, 1114 (1939). John Strong and Kenichi Watanabe, Phys. Rev., **57**, 1049 (1940).

independent of total pressure, whereas the infrared absorption by ozone is proportional to the fourth root of the total pressure. It follows that the ultraviolet and infrared measurements together determine the average total pressure on the ozone and so determine the average height of the ozone stratum.

THE ULTRAVIOLET MEASUREMENTS.

In the next parts of this paper the various measurements, the apparatus employed to make them, and the control and calibration of the apparatus will be described.

The ultraviolet measurements were made with two bands of radiation of about 6 Å width centered at 3050 and 3110 Å. The width and position of these bands are shown below in Fig. 3 in comparison with the mercury spectrum. The spacing of the two mercury lines 3125 and 3131 Å is to be com-

FIG. 3.

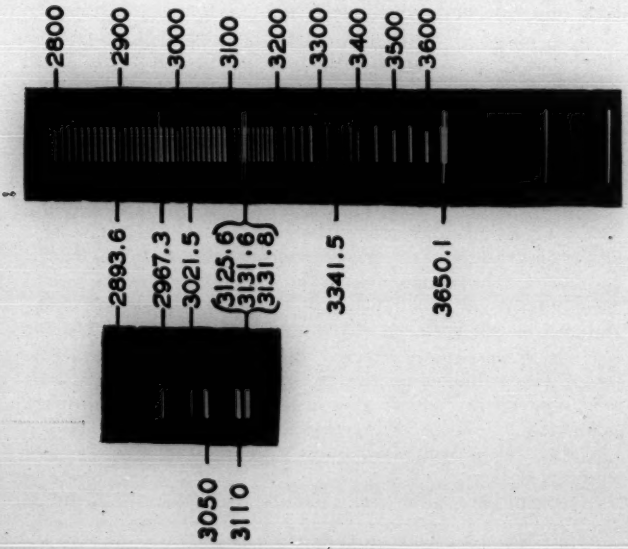

pared with the width of these two bands. These radiation bands at 3050 and 3110 Å were obtained with a Hilger-Müller double quartz monochromator. (The optical surfaces of this instrument were treated with a non-reflecting coat deposited by vacuum evaporation.[14])

To further illustrate the functioning of this monochromator Fig. 3, above, shows a series of monochromatic bands obtained with various settings of the wave-length drum. A mercury spectrum is superimposed for comparison. Both spectra in Fig. 3 were taken with a Hilger E-30 quartz spectrograph. The light emergent from the exit slit of the monochromator was focused on the entrance slit of the spectrograph with a concave aluminized mirror. An incandescent tungsten filament in a fused quartz envelope, focused on the entrance slit of the monochronomator, served as a continuous spectrum source.

For the solar measures the intensity of the light emergent from the exit slit of the monochronomator was determined with a sodium photocell in a quartz envelope. Fig. 4 shows the response of our apparatus as a function of wave-length with the sun as light source. For comparison we reproduce in Fig. 4 a microphotometer tracing of a solar spectrum taken on the flight of *Explorer II*.[9]

The general layout of our apparatus is shown in Fig. 5. This photograph was taken in the 48-inch Schmidt Telescope Dome on Palomar Mountain where the apparatus was set up. The sunlight falls directly on the clock mirror of the cœlostat which directs it onto the second cœlostat mirror. The second cœlostat mirror further reflects the sunlight toward the monochronomator and residual ray apparatus. The second cœlostat mirror affords both coarse manual adjustments, to get the light beam roughly directed, and the final fine adjustments, for guiding, achieved by electrical push buttons. These buttons control two small gear-head electric motors directly connected to the second cœlostat-mirror adjusting screws. The cœlostat mirrors are of glass with the front figured faces aluminized.

The sunlight is finally reflected and focused on the entrance

[14] John Strong, *J. O. S. A.*, **26**, 73 (1936).

FIG. 4.

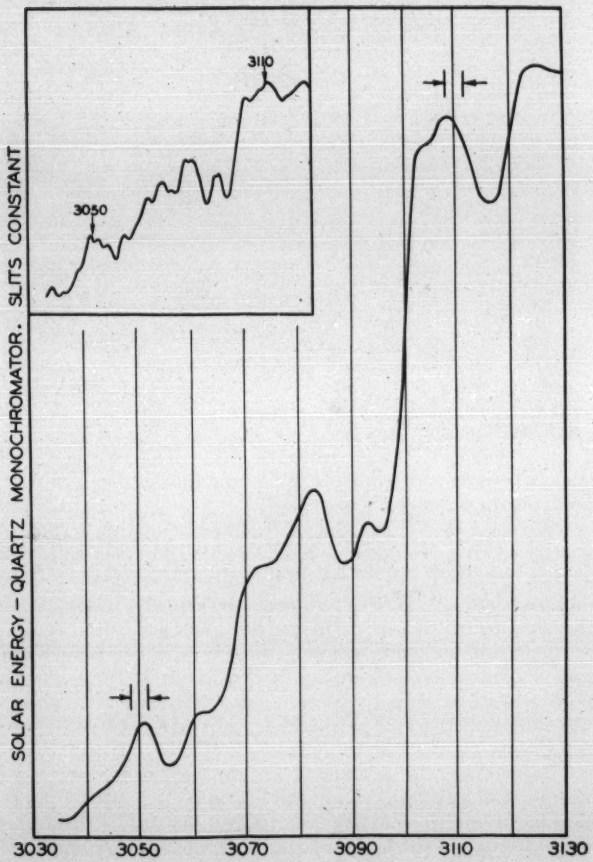
SOLAR ENERGY – QUARTZ MONOCHROMATOR. SLITS CONSTANT
3110
3050
3030
3050
3070
3090
3110
3130

FIG. 5.

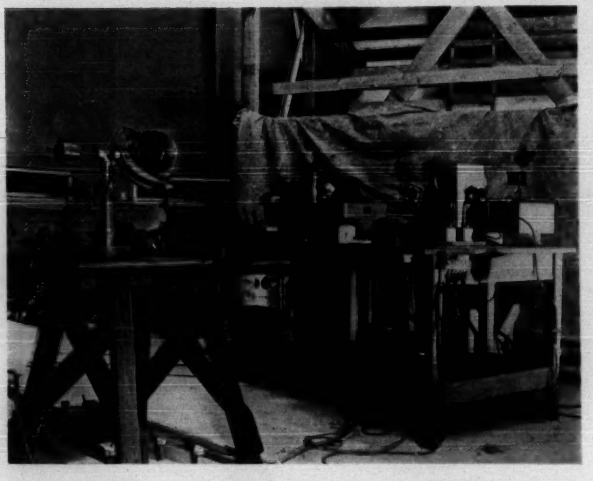

slit of the monochronomator by an aluminized concave parabolic mirror of 50 cm. focal length.

The light emergent from the monochronomator enters an evacuated chamber in which are: the sodium-quartz photocell, a D.C. amplifier tube (D-96475) and resistances of 10^6, 10^9 and 10^{11} ohms.[15] The amplified photocurrent produced by the sun, using the 10^9 ohm resistor, was measured with a portable galvanometer of 10^{-8} amperes per division sensitivity. Since the galvanometer deflection was not exactly proportional to the galvanometer current, a calibration curve was determined which was used to correct all galvanometer deflections.

To measure the amount of atmospheric ozone overhead, x_0, the sun was focused on the entrance slit of the monochromator and the galvanometer deflections at 3050 and 3110 were alternately read as the drum was rocked back and forth

[15] For a description and illustrations of this amplifier see "Procedures in Experimental Physics," pp. 422–3, Prentice-Hall, New York, 1938.

between limit stops. This was continued until five readings for each wave-length were determined. The time required was about one minute. Table II shows a typical set of these readings.

TABLE II.

Typical Ultraviolet Data Using the Sun as Source.

March 11, 1940	$h = 0^h\ 31\frac{1}{2}^m$
3050	3110
2.22	11.42
2.21	11.42
2.21	11.43
2.20	11.40
2.21	11.40
R (corrected) = 5.22	
Sec z = 1.27	

The amount of ozone overhead is determined from these readings by means of the following analysis in which:

I = observed deflection at 3110 Å,
I_0 = deflection one would get with no atmosphere,
I' = observed deflection at 3050 Å,
I_0' = deflection one would get with no atmosphere,
$R = I/I'$,
$R_0 = I_0/I_0'$,
x_0 = amount of ozone overhead expressed in cm. at N. T. P.,
z = zenith distance of the sun,
ζ = zenith distance of the sun at 22 k.m. as defined by Eq. 2,
α = optical density of 1 cm. ozone at 3110 Å,
α' = optical density of 1 cm. ozone at 3050 Å,
β = optical density of one air mass due to Rayleigh scattering at 3110 Å,
β' = same for 3050 Å,
δ = optical density of one air mass due to white haze and dust for 3110 Å,
δ' = same for 3050 Å.

We have

$$I = I_0\, 10^{-\alpha x_0 \sec\zeta - (\beta+\delta)\sec z} \qquad (5)$$

and

$$I' = I_0'\, 10^{-\alpha' x_0 \sec\zeta - (\beta'+\delta')\sec z} \qquad (6)$$

Dividing Eq. 5 by Eq. 6 and setting $\delta = \delta'$, which we do because scattering by haze may be regarded here as non-selective, we get

$$R = R_0\, 10^{-(\alpha-\alpha')x_0 \sec\zeta - (\beta-\beta')\sec z} \tag{7}$$

and

$$\log R - \log R_0 = (\alpha' - \alpha)x_0 \sec\zeta + (\beta' - \beta)\sec z. \tag{8}$$

R is the directly measured quantity in this equation. The other quantities are arrived at as follows: Guided principally by the work of Ny and Choong [16] we take

$$\alpha' - \alpha = 2.65 - 1.25 = 1.40\ \text{cm}^{-1}.$$

From the work of Cabannes and Dufay [5] we compute

$$\beta' - \beta = 0.415 - 0.384 = 0.03\ \text{atm.}^{-1}$$

Sec z was obtained at first by calculation from the equation of time, the latitude of the station and the ephemeris of the sun. Later, Sec z was determined from the tables of the Mount Wilson Observatory which were generously made available to us by Dr. Edison Pettit. At Palomar Mountain, it was necessary to apply a small correction to Pettit's tables to account for the difference in latitude and longitude between that station and Pasadena.

Sec ζ is obtained from sec z by applying Eq. 2.

Log R_0 is arrived at as follows. We have plotted the observed values of log R versus sec ζ for many days' observations. Fig. 6 shows the morning and afternoon measurements of October 14, 1939. From this plot, it appears that meteorological conditions were steady. The straight line of Fig. 6 extrapolated to "sec ζ = 0" yields log R_0 = − 0.160. Other plots yield other values of log R_0. Table III shows the values of log R_0 obtained on a set of days when meteorological conditions were judged to be steady. Aside from the fluctuations which may be ascribed to changing meteorological conditions the obtained values of log R_0 depend on the constancy of the sun and of the instrument. As for the latter,

[16] Ny-Tsi-Zé and Choong-Shin-Piaw, *Chinese J. Phys.*, 1, 1 (1933).

FIG. 6.

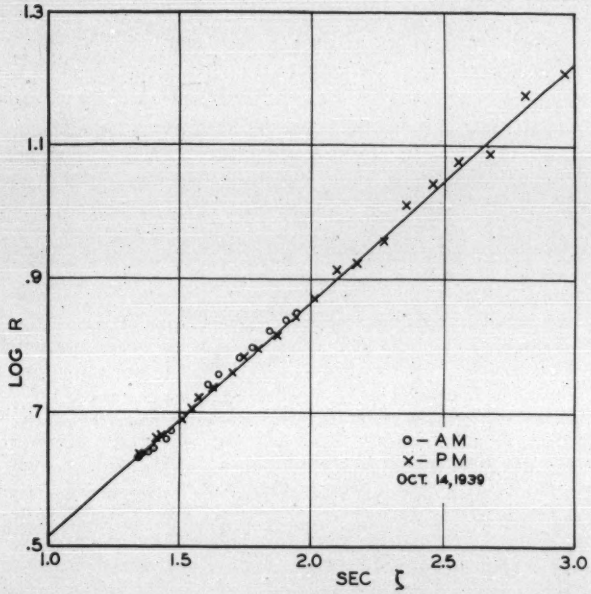

TABLE III.

Selected Values of log R_0.

	No. of Points.	$-\log R_0$
October 4, 1939	41	.134
5	21	.164
9	21	.175
10	42	.164
11	39	.159
12	29	.144
13	25	.176
14	38	.160
16	36	.191
23	22	.182
	Weighted Mean	.167

R is observed to change about 1 per cent. for a deliberate change of 1 Å in the wave-length settings. We have kept the wave-lengths properly positioned by frequently mapping the spectrum as shown in Fig. 4. The final chosen value of $\log R_0$ was

$$\log R_0 = -0.167,$$

With this value of $\log R_0$ we are now prepared to apply Eq. 8 to the interpretation of the observed ratio of the galvanometer deflections, R and determine the amount of ozone overhead. We get

$$x_0 = \frac{\log R - 0.167 - 0.03 \sec z}{1.4 \sec \zeta}. \qquad (9)$$

WATER VAPOR DETERMINATION.

Figure 7 shows the near infrared solar spectrum obtained

FIG. 7.

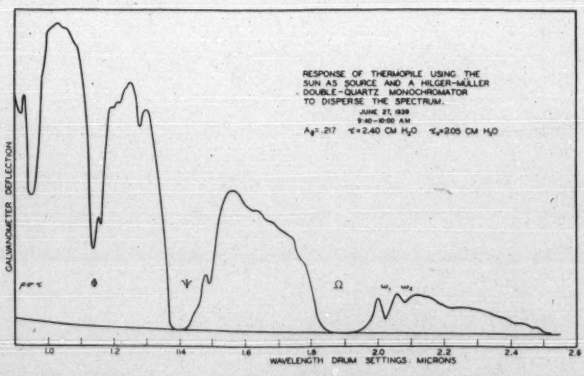

with the Hilger-Müller double-quartz monochromator. The telluric absorption bands are labelled, using Langley's notation. Of the water vapor absorption bands shown there the Φ-band was used to determine the amount of water vapor overhead.

The same cœlostat and focusing mirror described above were used to focus the sun's image on the entrance slit of the monochromator. For the Φ-band measurement, as contrasted with the ultraviolet measurement, a diaphragm was interposed immediately in front of the entrance slit of the monochromator. The diaphragm had an aperture equal to about one-third that of the solar image and its function was to make the solar energy entering the slit independent of small errors of guiding of the solar beam.

A small 45° mirror placed in the emergent radiation from the monochromator directed the radiation laterally onto a quartz lens which in turn focused it on a Kipp and Zonen thermopile. This thermopile was connected through a double-pole, double-throw switch to a L. and N. type HS galvanometer. The galvanometer deflection was read by means of a translucent glass scale on which the reflected and focused image of a straight filament lamp played. The galvanometer scale appears in Fig. 5.

Figure 8 shows the Φ-band as measured at Pasadena on two occasions, one when there was very little water vapor overhead and the other for more water vapor. The absorption by this band, A_Φ, is, following Fowle, the ratio of the area $a\,b\,c\,a$ to $a\,c\,d\,e\,a$. The band limits are 1.05 and 1.25 μ. We use Fowle's[17] calibration curve to connect A_Φ with the amount of water vapor, τ, penetrated by the solar beam.

In routine measurements of A_Φ, the slits were widened to give a smooth curve and instead of integrating the areas $a\,b\,c\,a$ and $a\,c\,d\,e\,a$ with a planimeter, the galvanometer deflections were reduced by an equivalent algebraic process.

The relation between τ and the amount of water vapor overhead, τ_0, is,

$$\tau = \tau_0 \sec z. \qquad (10)$$

THE FAR INFRARED MEASUREMENTS.

Figure 9 is a grating-energy curve of the sun showing the absorption by the 9.6 μ band of ozone. Superimposed on this curve is the wave-length response curve of a five-crystal residual-ray apparatus fitted with apophyllite crystals. The half-width of this response band is 0.34 μ and the maximum

[17] F. E. Fowle, *Smithsonian Misc. Coll.*, **68**, No. 8 (1917).

FIG. 8.

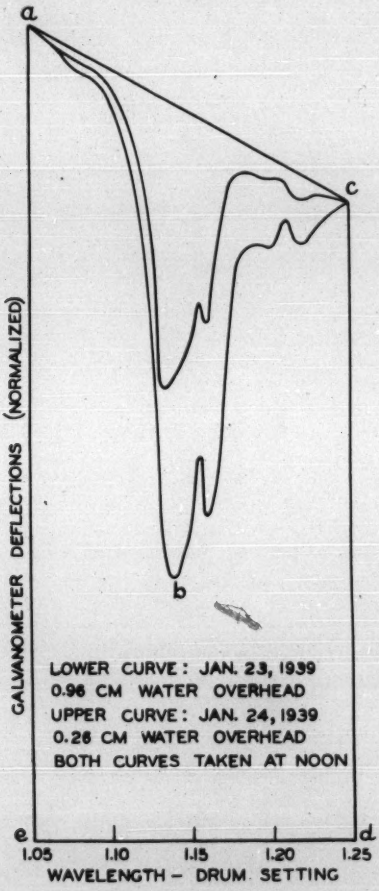
a
b
c
d
e
GALVANOMETER DEFLECTIONS (NORMALIZED)
LOWER CURVE: JAN. 23, 1939
0.96 CM WATER OVERHEAD
UPPER CURVE: JAN. 24, 1939
0.26 CM WATER OVERHEAD
BOTH CURVES TAKEN AT NOON
1.05
1.10
1.15
1.20
1.25
WAVELENGTH – DRUM SETTING

FIG. 9.

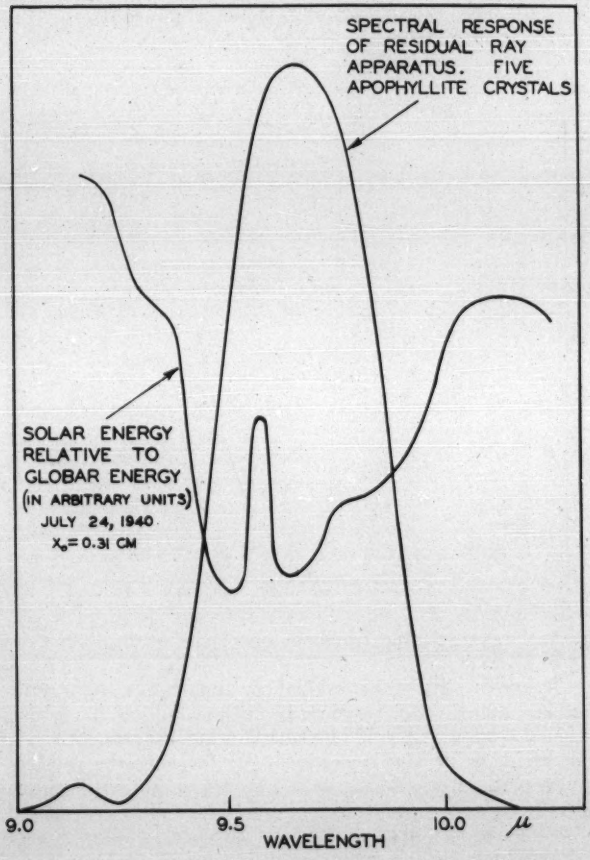
SPECTRAL RESPONSE
OF RESIDUAL RAY
APPARATUS. FIVE
APOPHYLLITE CRYSTALS
SOLAR ENERGY
RELATIVE TO
GLOBAR ENERGY
(IN ARBITRARY UNITS)
JULY 24, 1940
X_o = 0.31 CM
9.0
9.5
10.0
μ
WAVELENGTH

response is centered at 9.66 μ. The grating spectrometer employed to obtain these curves as well as the residual-ray apparatus have been described in a previous publication.[18] Fig. 10, from this publication, shows the response of other

FIG. 10.

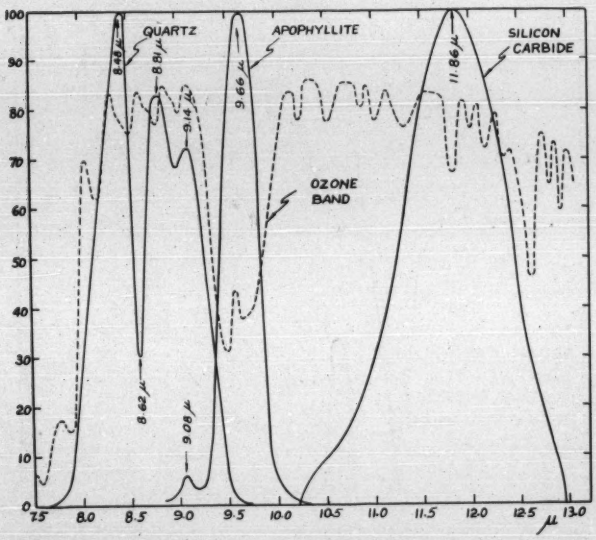

residual rays and the transmission of the atmosphere from 7.5 to 13 μ.

The sensitivity of the residual ray apparatus to solar radiation is confined to the response band shown in Fig. 9. This is evident from the result of the following experiment. The galvanometer deflection produced by focusing the residual-ray apparatus on the sun was tested first with the optical path open and second, with a thin glass plate interposed. Such a glass plate transmits freely the visible and near infrared radiations which comprise almost all of the total solar

[18] John Strong, *J. O. S. A.*, **29**, 520 (1939).

radiation, but it is opaque to the 9.6 μ band. The galvanometer deflection produced by the short wave-length solar radiation, through the glass plate, was only 0.25 per cent. of the deflection obtained with the optical path open.

The solar observations at 9.6 μ were made according to the following regime. By means of the push buttons, the second cœlostat mirror was caused to raise the solar beam from the 50 cm. focus mirror up onto the focusing mirror of the residual-ray apparatus. The image of the sun formed by this mirror more than covered the entrance aperture of the residual-ray apparatus. A wooden shutter interrupted the beam during each odd half minute. The thermocouple of the residual-ray apparatus was connected to the L. and N. type HS galvanometer through the double-pole double-throw switch. After reading several galvanometer deflections, $d_\odot$, the residual-ray apparatus was directed and focused on a comparison globar source. The deflections produced by this source, d_G, allowed the solar energy received to be expressed in terms of the energy received from the globar thus eliminating the influence of variations of the sensitivity of the residual-ray apparatus. The absolute temperature of the globar, θ, was measured and frequently checked with an optical pyrometer. This temperature was regulated and kept nearly constant by means of two parallel-connected iron-filament ballast tubes (UV-876).

W, the solar energy received, expressed in cal cm^{-2} sec^{-1}, is obtained from Planck's equation:

$$W = \Omega_\odot \frac{0.34 \times 10^{-4} \times 2.81 \times 10^{-13}}{(9.66 \times 10^{-4})^5} \left(\frac{1}{e^{\frac{1432}{9.66\theta}} - 1} \right) \frac{d_\odot}{d_G} \qquad (11)$$

or more briefly

$$W = C \left(\frac{1}{e^{\frac{1432}{9.66\theta}} - 1} \right) \frac{d_\odot}{d_G}, \qquad (12)$$

where $\Omega_\odot$ is the solid angle subtended by the sun. In this calculation, the globar is assumed to be a black body at both wave-length regions; at 9.6 μ for the residual-ray measurement and at 6000 Å for the θ measurement. The values given for W are contingent on the validity of these assumptions.

Before one can get from W the ozone absorption, A_τ, it is necessary first to correct W to account for the absorption of water vapor at 9.6 μ. This yields W'. Also one must know the value W' would have if there were no ozone in the atmosphere. Let us call this last quantity W_0.

The transmission of the atmosphere at 9.6 μ as it relates to water vapor absorption is $10^{-0.052\tau}$. We have already described the method by which the amount of water penetrated by the solar beam, τ, is determined from the measurement of A_ϕ. The absorption at 9.6 μ is considered here to be exponential [19] in character. The above value of 0.052 for the optical density of 1 cm. of water vapor is calculated from the published measurements of Adel.[20] Thus we have

$$W' = W10^{0.052\tau}. \qquad (13)$$

To determine W_0, one plots W' as a function of the square root of x, the amount of ozone penetrated. This plot is substantially a straight line which is extrapolated to $x = 0$. From many such plots, those were selected which appeared to correspond to the most stable meteorological conditions and from these the final mean extrapolated value of W_0 was obtained.

$$W_0 = 3.0C.$$

The absorption by ozone at 9.6 μ is, accordingly,

$$A_\tau = \frac{W_0 - W'}{W_0}. \qquad (14)$$

The final data which are required to determine the total pressure on the atmospheric ozone are A_τ and x. But, to interpret these data it was necessary to establish the relationship between P, A_τ and x by a series of laboratory calibration tests.

LABORATORY CALIBRATION OF THE 9.6 μ OZONE BAND.

Measurements of A_τ and x for ozone-oxygen mixtures were made with the apparatus shown diagrammatically in

[19] W. M. Elsasser, *Astrophys. J.*, **87**, 497 (1938).
[20] Arthur Adel, *Astrophys. J.*, **89**, 1 (1939).

Fig. 11 at the following total pressures; 722, 194, 104, 58, 26, 13 and 6 mm. of mercury.

The regime of this calibration was to fill the cell of Fig. 11 with an ozone-oxygen mixture at one of the prescribed pressures and periodically to make a complete set of observations of A_r and x as the ozone decayed. The results of these calibration tests are shown graphically in Fig. 12. The general consistency of the measurements is indicated in this plot,

FIG. 11.

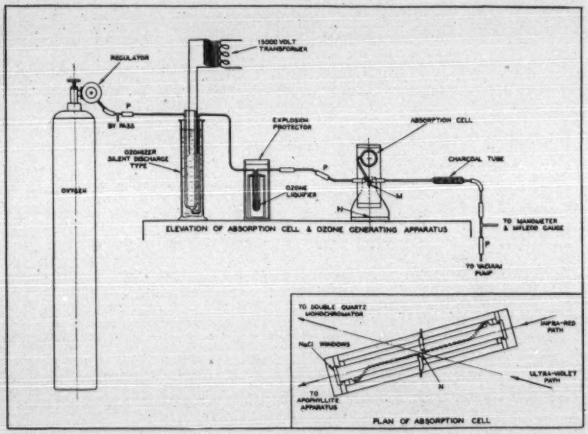

where the curve for each pressure is defined by at least two sets of interspaced points representing separate cell fillings.

The insert in Fig. 11 shows in plan how the absorption cell was arranged with respect to the infrared and ultraviolet optical paths. The cell was made of glass. It was 3 inches in diameter and 36 inches long. The ends of the cell were fitted with optically worked NaCl windows. The cell pivoted, in a wooden frame, in which it was mounted, about a vertical axis N to swing into a position parallel with either the infrared or the ultraviolet optical path. The wooden frame in

FIG. 12.

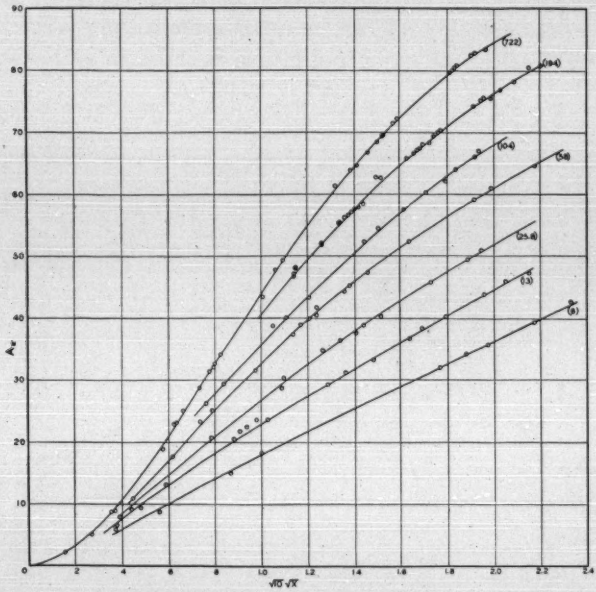

either of these positions could be rotated about an axis M so as to be "in" or "out" of the optical path.

The infrared absorption A_τ was measured with collimated radiation from a globar source using the residual-ray apparatus with apophyllite crystals as receiver. "In" and "out" measurements were made of the globar intensity and the ratio of these measurements yielded $T_\tau \times T_c$ where $T_\tau = 1 - A_\tau$ and T_c is the transmission of the NaCl windows. T_c was measured from time to time with the cell evacuated and found to be always nearly 0.83.

The measurement of x was made with the help of the Hilger-Müller monochronomator with photocell receiver using the wave-lengths 3050 and 3110 Å. The source of ultraviolet radiation was, as before, an incandescent tungsten filament in

a quartz envelope. The ultraviolet radiation was focused and collimated with quartz lenses.

Let R be the ratio of the observed deflection at 3110 to that at 3050 Å with the cell "in." Let R_0 be the same ratio with the cell "out." The correction of R for the rocksalt windows is made by means of the measured factor 1.024. The amount of ozone in the cell expressed as centimeters path length at N. T. P. is given by

$$x = \frac{\log (R \times 1.024) - \log R_0}{1.40}. \qquad (16)$$

R_0 was frequently measured as a control. Its value was found to be very constant owing to the fact that the tungsten lamp current was controlled by a Raytheon regulator.

Table IV reproduces one complete set of observations.

TABLE IV.

Typical Data for Calibrating the Pressure Effect on the 9.6 μ Fundamental Oscillation-rotation Band of Ozone.

(Martin Summerfield observer.)

Time.	UV: Off IR: Off	3050 In	Off Off	3110 Out	Calculations.		
2:36	−.08	2.41	−.07	9.78	2.485	9.830	$T_\pi \times T_c =$
	−.03	2.43	−.04	9.79	2.465	9.815	$\frac{2.481}{9.815} = .2528$
I–R	−.01	2.48	−.01	9.80	2.490	9.800	
	+.01	2.49	00		2.485		
2:49	−.17	2.33	−.22	8.08	2.525	8.275	R =
	−.17	2.38	−.18	8.07	2.555	8.240	$\frac{8.268}{2.546} = 3.248$
U–V	−.16	2.38	−.19	8.13	2.555	8.290	
	−.13	2.39	−.19		2.550		
3:06	+.06	6.53	+.07	9.90	6.465	9.825	$R_0 =$
	+.08	6.49	+.07	9.84	6.415	9.745	$\frac{9.797}{6.414} = 1.528$
U–V	+.12	6.47	+.09	9.91	6.365	9.815	
	+.10	6.50	+.08		6.410		
3:22	+.00	2.57	−.02	8.33	2.580	8.335	$R =$
	+.01	2.58	−.02	8.37	2.585	8.365	$\frac{8.363}{2.581} = 3.240$
U–V	+.03	2.58	−.03	8.39	2.580	8.390	
	+.03	2.58	−.03		2.580		
3:40	−.08	2.43	−.09	9.70	2.515	9.785	$T_\pi \times T_c =$
	−.08	2.44	−.08	9.70	2.520	9.780	$\frac{2.518}{9.783} = .2572$
	−.08	2.44	−.08		2.520		
3:50	Pressure: 819 + 88 − 184 = 723 mm. Temperature: 83° F.						

The increase of the $T_r \times T_c$ values of Table IV and the decrease of the R is due to the decay of ozone. In using these results the two infrared transmissions and the two ultraviolet ratios were averaged and the averages were assigned to the time of the R_0 determination. The total time to take a complete set of observations was about one hour and such a set yields one point on the final calibrations curve (Fig. 12).

Incidentally, values of $1/x$ plotted against time gave a nearly straight line showing that the decay of ozone was, in the main, a bimolecular reaction.

For total pressures of 26 mm. and higher, the cell was filled with ordinary tank oxygen ($99 O_2 : 4 N_2$) which was passed through the silent discharge ozonizer. The starting amount of ozone was adjusted to $x \sim 0.5$ cm. The total pressures were determined by means of a mercury manometer.

For total pressures of 26 mm. and lower, pure ozone was first admitted into the cell. The pure ozone was separated from the oxygen-ozone mixture, produced by the ozonizer, in a preliminary step by means of a trap cooled with liquid air. Later the pure ozone was boiled off into the cell. Then the total pressure was adjusted to the desired value by adding tank oxygen. Total pressures of 26 mm. and lower were measured with a McLeod gauge.

Koroseal tubing [21] served to make all flexible connections and, with pinch clamps, served also to make the connections P shown in Fig. 11 which were closed and opened. Mercury in the pressure gauges was protected from tarnishing by a charcoal trap inserted to remove ozone.

Log A_r is plotted against log P in Fig. 13 for $x = 0.05$, 0.1, 0.2, 0.3 and 0.4 cm. of ozone. We see in this plot that A_r is substantially proportional to $P^{1/4}$. The dashed lines in Fig. 13 have a slope equal to 1/4.

PRESSURE EFFECT OF ULTRAVIOLET ABSORPTION.

Among those who have tested the pressure effect of ultraviolet absorption is Vassy [22] who states, "A first tube 8.8 cm. long, in line with two others of the same diameter as the first

[21] John Strong, *Rev. Sci. Instruments*, 10, 104 (1939).

[22] E. Vassy, "Conference on Atmospheric Ozone Held at Oxford, September 9 to 11, 1936," p. 26, published by the Royal Meteorological Society; London, 1936.

FIG. 13.

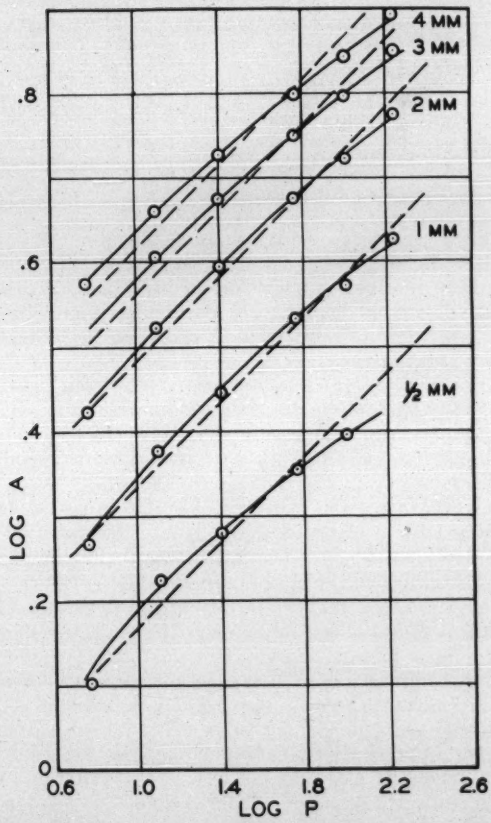

and respectively 1 meter and 2.53 meters long, contains a mixture of oxygen-ozone under normal pressure; the two other tubes are at first evacuated. The three tubes are traversed by a parallel beam of light issued from a hydrogen

tube. A spectrum is taken, and the mixture is made to expand into the two other tubes. (This was made in two times to prevent explosions.) Then another spectrum is taken, which was proved by microphotometric measurement to be identical with the first.

". . . The ratio of pressure was 1/40; the lower pressure was the pressure in the atmosphere at a height of about 27 k.m., i.e. slightly above the center of gravity of atmospheric ozone. Therefore, it is not necessary to consider pressure effect in measurements concerning the thickness of the ozone layer."

This conclusion is, indeed, what we might expect considering that the rotational detail of the ozone absorption has never been resolved in the solar spectrum and further, that the Hartley band exhibits an abnormally high absorption coefficient—the optical density of ozone in the center of the Hartley band (at 2553 Å) is $\alpha = 63$ (a layer of ozone gas at N. T. P. of only .002" thickness reduces incident light to 1/2 its value). High absorption in molecular bands is associated with diffusiveness of structure and this in turn implies that the absorption will follow Beer's law and be independent of total pressure.

However, since the existence of a zero pressure effect in the ultraviolet is of primary importance for the application of the new method of measuring the height of the ozone, it seemed desirable to get further experimental evidence.

The glass absorption cell shown in Fig. 14 was used to get evidence. This cell was two inches in diameter and forty inches long. It was fitted with two quartz windows, an attached pumping line with oxygen generator, two vents for admitting nitrogen to raise the total pressure in the cell, and an electrode and depending glass tube for generating and collecting liquid ozone by Goldstein's method.[23]

The regime of measurement was to evacuate the cell and clean it with a discharge. Then oxygen was generated by heating $KMnO_4$ until about 0.15 cm. of mercury pressure was attained. The cell was then sealed off at B in such a manner as to afford a capillary vent for later readmitting gas.

[23] E. Goldstein, *Ber. d. Deutsch. chem. Gesellsch.*, 36, 3042 (1903).

At this stage measurements of the intensities of the light at 3110 and 3050 Å penetrating the cell were started. The aforementioned regulated tungsten lamp served as the light source and the Hilger-Müller monochromator with its auxiliary apparatus was used to isolate and measure the two wavelength bands. The ozone trap was next cooled to about 60° K., by means of fresh liquid air boiling under vacuum, and a high frequency discharge was started between the electrode and a metal foil wrapped around the depending tube. Intensity measurements were continued (See Table V). After about an hour, the discharge was stopped, the vacuum pump to the liquid air was stopped, and later, the

FIG. 14.

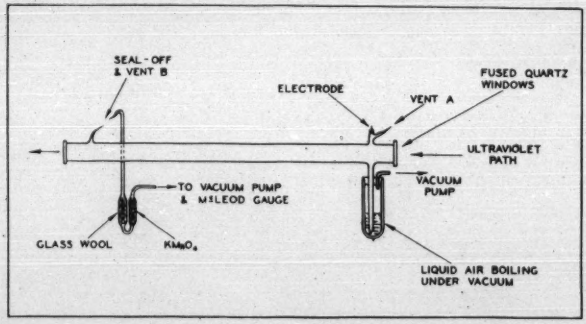

liquid air was removed. At this stage the collected ozone evaporated into the absorption cell as the measurements given in Table V show. The decay of ozone was followed by optical measurement for a time to determine the decay curve. Then pure tank nitrogen was admitted through vent *A* until the pressure in the cell was about 1/2 atmosphere. Vent *A* was then sealed and the pressure raised to 1 atmosphere by admitting nitrogen through vent *B*. After this, vent *B* was sealed. The ultraviolet intensities were again determined and, after allowing for further "decay," the cell was finally evacuated to determine how nearly the original conditions were reproduced.

Three experiments were conducted and all gave substantially the same result as the one reported in Table V.

If Beer's Law is not followed one would expect an increase of absorption coefficients (especially since the pressure is increased 750 fold). Actually, it appears that there was an evanescent decrease. This temporary apparent decrease in α is explained as a decrease in x owing to a crowding of the ozone away from the center of the tube toward the walls and out of the optical beam. It will be noted that in conformity with this hypothesis there is a later increase of x (apparently due to diffusion) from .079 cm. to .091 cm.

TABLE V.

Effect of Increasing Total Pressure on O_3 from 1 mm. to 750 mm.

Time.	I_{3110}.	I_{3050}.	$\log \frac{I_{3110}}{I'_{3110}}$	$\log \frac{I_{3050}}{I'_{3050}}$	$\log \frac{R}{R_0}$.	x_{3110}.	x_{3050}.	x_R.	Remarks.
2:00	17.40	11.56							$P_{O_2} \leqq 1.5$ mm.
2:10	17.23	11.47							Trap cold, spark on.
3:30	16.87	11.28							Spark off.
3:45	16.67	11.09							Vacuum off tap.
3:59	12.14	5.56	.1432	.3060	.1646	.114	.116	.118	Liquid air off tap.
4:23	12.41	5.87	.1297	.2787	.1508	.104	.105	.108	Decaying
4:45	12.60	6.10	.1192	.2588	.1408	.095	.097	.101	Decaying
4:51	12.77	6.53	.1123	.2281	.1166	.090	.086	.083	Let in N_2
5:02	12.71	6.34	.1126	.2393	.1106	.090	.090	.079	Cell sealed.
5:18	12.58	6.27	.1092	.2370	.1277	.087	.089	.091	Decay
5:26	16.10	10.77							Cell evacuated.

Note: I'_{3110} and I'_{3050} were obtained by interpolation between 2:00 and 5:26 data. α_{3110} taken as 1.25; α_{3050} taken as 2.65; $\alpha_{3050} - \alpha_{3110} = 1.40$.

REDUCTION OF MEASUREMENTS.

The final data required to determine the height of the ozone are A_r and x or $\sqrt{x}$ together with the calibration data of Fig. 12. The method we followed of reducing the measurements of a single day is described below.

For each day the values of the quantity $10^{0.052r}$ were calculated from the Φ-band measurements and plotted as a function of the hour angle of the sun.

The values of $\sqrt{x}$ were calculated from R' and also plotted as a function of the hour angle of the sun.

Likewise, values of d_o were plotted as a function of the hour angle of the sun.

Three curves were drawn through the above three sets of points and from them interpolated values of the three quantities were determined for the hour angles corresponding to the residual-ray measurements of $d\odot$. Using Eqs. 12, 13 and 14, the final data $\sqrt{x}$ and A_r were obtained and plotted as ordinates and abscissa respectively on translucent graph paper.

This plot was laid in register over a master curve sheet on which was plotted A_r vs. $\sqrt{x}$ curves for each kilometer of height from 15 to 29 km. (See Fig. 15.) These curves were

FIG. 15.

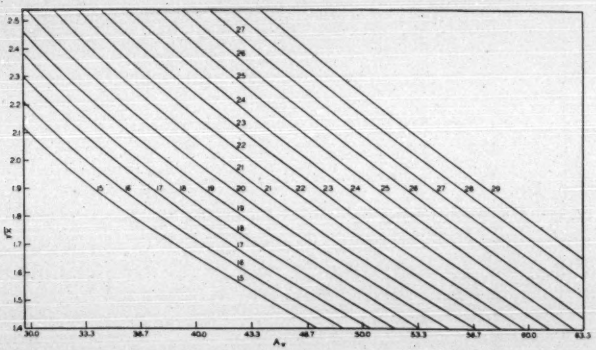

obtained from the calibration data (Fig. 12) and the pressure-height relation in the upper atmosphere given by Chapman and Milne.[24] The height corresponding to each plotted A_r value is determined from the master sheet to the tenth of a kilometer.

These heights are plotted as a function of hour angle together with the total ozone and water vapor overhead, as shown in Fig. 16. The days given in this figure represent Palomar observations. The observations at Pasadena and a discussion of all observations will be given in a subsequent

[24] S. Chapman and E. A. Milne, *Quart. Jour. Roy. Met. Soc.*, 46, 357 (1920).

FIG. 16.

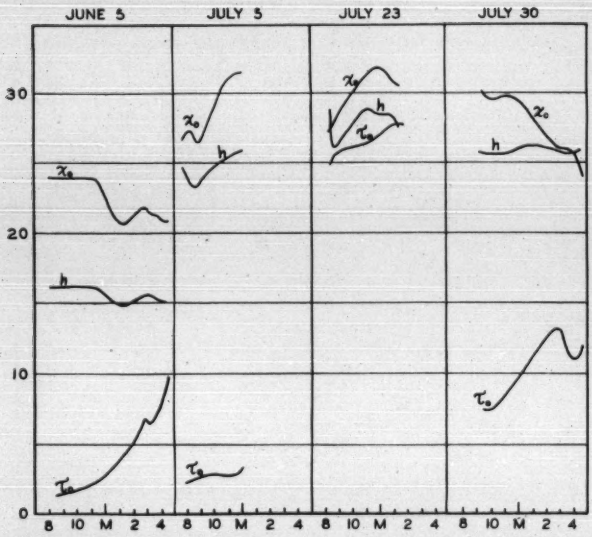

publication. The ordinates of Fig. 16 are to be multiplied by 10^{-2} cm for x_0, by 10^{-1} cm for τ_0, and by 1 km for h.

CONCLUSION.

The pressure which we obtain is an average pressure. It is related approximately with the vertical distribution of ozone (as determined by the balloon method) by the following formula:

$$P = \left\{ \frac{\int_0^\infty [O_3] P^{1/4} dh}{\int_0^\infty [O_3] dh} \right\}^4. \qquad (17)$$

The values of h that we get of about 25 km. are higher than previous values. This was somewhat unexpected in view of the character of weighting.

The present method of measuring the height is subject to several uncertainties.

First, the effect of a total pressure obtained by means of an ozone rich mixture of oxygen is taken to be the same as the effect of a total pressure produced by stratosphere air in which the ozone concentration is very small.

Secondly, the effect of temperature is entirely neglected. The calibration experiments were conducted at about 27° C., whereas the ozone in the stratosphere exists at sub-zero temperatures. The cooling of ozone to a lower temperature will modify the distribution of intensity in the π-band.

A third possible source of error is in the determination of W_0. This quantity is assumed to be constant from day to day, and it is believed the value 3 C. is not in error by more than 10 per cent.

The pressure effect on the Φ-band and the pressure effect of water absorption at 9.6 μ have been ignored. This is justifiable only if these pressure effects are the same. If these pressure effects are the same, τ represents a spectroscopically significant thickness and that is exactly what we wish for substitution in the expression $10^{0.052\tau}$.

It should be noted that the method as applied here uses an apparatus which operates on a preselected wave-length band at 9.6 μ and the method assumes constancy of the solar emission. There are several possibilities of improving the determination of A_τ and these are now being explored.

In conclusion I wish to acknowledge the helpful collaboration of Dr. Kenichi Watanabe who, in addition to assisting in the development of this method, has made measurements both at Pasadena and on Palomar Mountain over an extended period of time which are the subject of a forthcoming paper by him.

I wish to acknowledge my gratitude to Mr. Marcus H. Brown and Mr. Raymond L. Chaplin for preparing the optical surfaces for the apparatus and for making the rocksalt windows.

Better Coverage.—(*General Electric Review*, Vol. 43, No. 10.) Under certain conditions, the area of good radio broadcast service with frequency-modulated transmission is 33 times greater than with amplitude, or present-type broadcasting, according to test and calculations made by General Electric radio engineers. The tests also show that receivers located between the service areas of two frequency-modulated stations can get either station by means of a directional antenna. Thus vast AM interference areas can be converted into "discriminating" areas by the use of FM. The tests give added proof that FM permits more stations to operate on the same channel by reducing the distance required between stations. At the same time these stations can give good reception over a much greater area than was previously possible with amplitude modulation, and can do so with lower power.

R. H. O.

Air Conditioning May Halt Decentralization in Cities.—(*Heating, Piping and Air Conditioning*, Vol. 12, No. 10.) Modern office building construction with conditioned air free of dirt and smoke, and artificial light that rivals the natural product, may offer the specific necessary to offset the decentralization of downtown business districts with the accompanying expensive obsolescence of downtown properties. This is the conclusion of E. M. McConney, vice-president and actuary of the Bankers Life Co., Des Moines, Iowa. Mr. McConney served as chairman of the building committee responsible for the location and erection of the company's $2,000,000 home office building completed this past summer near the heart of the Des Moines business district. Mr. McConney said Bankers Life considered both a suburban and a downtown site, but decided in favor of the downtown location "because air conditioning is looked upon as an economical necessity and that solves the problem of smoke and dirt." Double glazed windows, never opened except for cleaning, keep out dirt. Two inches of cork insulation from basement to roof insulate the building against noise as well as heat and cold losses. As a result, Mr. McConney contends, the downtown location has all the advantages of a suburban site save one—parking convenience.

R. H. O.

NATURAL FREQUENCIES OF THREE PHASE WINDINGS.

BY

REINHOLD RÜDENBERG, Dr.Ing., Dr.hon.,

Graduate School of Engineering
Harvard University
Cambridge, Mass.

1. INTRODUCTION.

The natural oscillations of electric power circuits play an important part in the operation of systems under many practical conditions. Particularly when interrupting short-circuit currents these oscillations determine the interrupting capacity of the circuit breaker and therefore may decide the maintenance of the power supply. Because of the complexity of modern power networks it is not easy to predict the behavior of such oscillations, and their dependence on the various parameters of the system has been investigated only slightly up to the present time.

We will determine here the natural frequencies of simple three-phase circuits, as these form the elements of every important power system. According to the various cases, however, which occur in actual operation, we shall consider star as well as delta connection, insulated as well as grounded condition of the poles, and we shall take account of the connection of the grounded pole with the first as well as with the last interrupted arc within the three-phase circuit breaker. Although our investigation is valid for overhead lines or underground cables as well as for generators, motors, transformers and reactors, we will specify for the most part windings working either in star or in delta connection.

In windings as well as in smooth lines the natural oscillations are determined by the interaction of the distributed self-inductance and capacitance. This involves a wave-like propagation of current and voltage along the line or winding with a definite velocity. In contrast to the high velocities of $300m/\mu s$ for overhead lines and $150m/\mu s$ for underground cables many measurements show that the order of the wave

velocity along the wire in transformers is about $100m/\mu s$ and in machines about $30m/\mu s$. Theoretically this velocity can be determined for every case as

$$v = \frac{1}{\sqrt{lc}}, \qquad (1)$$

where l is the effective self-inductance and c is the effective capacitance, both per unit length. Although the internal turn-capacitance and also the coil-capacitance of windings tend to diminish the wave velocity, we will assume in this paper that the velocity is known for every case.

The natural oscillations are then produced by repeated reflections of the travelling waves at the ends of the winding and their frequency can be derived from the length of the winding. If we consider initial waves of nearly rectangular shape, the frequency of the higher harmonics even may be so determined. However, by action of the continuous flattening of these waves within the windings the very high harmonics disappear.

In three-phase windings the single phases are coupled together mainly by their conductive connection either at the star point or at the delta corners. This coupling has a fundamental influence on the frequency of the oscillations. Besides this conductive coupling there is slight capacitive and inductive coupling between the phase windings, for example within the overhang of an alternator, or between the coils on different limbs of a transformer. We will neglect this, however, because it is of secondary influence. In the same way, we will not consider here the influence of any additional capacitance at the terminals of the winding, which may be caused by terminal bushings, by connecting cables or the like, since it can easily be treated separately.

The natural oscillations and frequencies can be calculated in a fairly simple way by considering the travelling waves of voltage caused by the instantaneous interruption of a short-circuit current within the winding, which is similar to the most important practical problem. This enables us to develop a relatively simple solution for the various actually existing conditions of operation and this solution agrees closely with experimental results.

2. SINGLE-PHASE WINDINGS.

To clarify our method of investigation we will begin with the well-known case of interrupting a short-circuit current in a single winding of a source of current, as in Fig. 1. If the

FIG. 1.

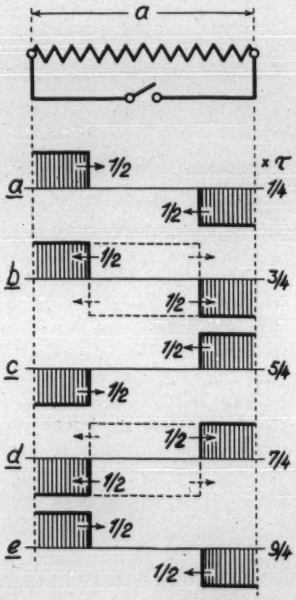

Interruption of the short circuit of a single-phase winding in insulated state.

winding is symmetrical, half the interruption voltage appears at each end but with opposite sign. Each rectangular voltage wave travels over the whole line, undisturbed by the other wave, the full lines in Fig. 1 representing the resultant voltage. The successive pictures of Fig. 1*a–e* represent the voltage distribution over the line after 1/4, 3/4, 5/4, etc. of the travelling time

$$\tau = \frac{a}{v}, \qquad (2)$$

which the waves require to pass once through the whole length a of the phase winding. After 8/4 of this time τ the original distribution repeats itself, and therefore the period of the phenomenon is 2τ and its frequency is, therefore,

$$f_0 = \frac{v}{2a}. \tag{3}$$

We see that to attain this result it is sufficient to follow the progress of any of the steep wave fronts which are reflected at the open ends of the winding without change of sign. Every front, therefore, regains its initial position after travelling a distance $2a$, giving at once equation (3) for the natural frequency.

If one pole of the single-phase winding is grounded, then for the interruption of a short-circuit we have the diagram of Fig. 2. Now the entire voltage appears at the interrupted open end and travels in a steep front over the winding. The other terminal, which is connected to ground, represents a short-circuited end and here every wave is reflected with change of sign. So the successive distributions of voltage in Fig. 2*a–e* occur after 1/4, 5/4, 9/4, etc. of the travelling time τ and we see that the initial distribution is repeated only after 4τ. The steep front has to travel over a distance $4a$ and in this case the natural frequency is

$$f_0' = \frac{v}{4a}. \tag{4}$$

Because voltage waves cannot penetrate through any short circuit point, we may have beyond the left-hand end of Fig. 2 any other winding, for example two additional phase windings of a star-connected three-phase system. We see, therefore, that we have obtained in equation (4) also the natural frequency of a three-phase system with grounded neutral.

It is well known that in the case of Fig. 1, with two open ends of the line, besides the fundamental frequency of equation (3) a series of harmonics with higher frequencies h may be present, which are integral multiples of the fundamental frequency. The whole series of frequencies which compose

the wave shapes of Fig. 1 is given therefore by

$$\frac{h}{f_0} = 1, 2, 3, 4 \cdots. \tag{5}$$

In the case of Fig. 2, with one end open and one end short-circuited, higher harmonics may occur which are odd multiples

FIG. 2.

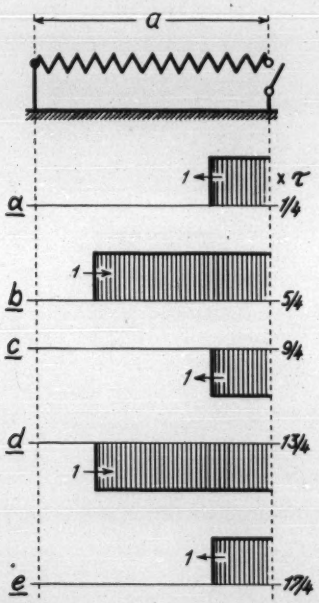

Interruption of the short circuit of a single-phase winding in grounded state.

only of the fundamental frequency of equation (4), namely

$$\frac{h}{f_0'} = 1, 3, 5, 7, \cdots \tag{6}$$

and which together form the rectangular shapes of Fig. 2.

The existence of such higher frequencies enters in all cases which are investigated later.

3. INTERRUPTION VOLTAGE IN HETEROGENEOUS CIRCUITS.

The initial distribution of voltage after interruption of a short circuit in three-phase systems is different from that in Fig. 1 or 2, because several phase windings act in parallel and disturb the symmetry of the winding ends. The general scheme of interruption is represented in Fig. 3. E and I are

FIG. 3.

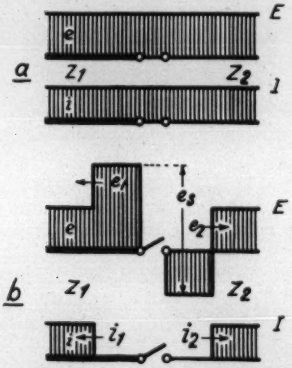

Production of interruption-voltage at the junction of heterogeneous lines.

voltage and current immediately before the interruption. In the neighborhood of the circuit breaker they are spatially constant as in Fig. 3*a*. Immediately after the interruption the current I vanishes and therefore receding wave steps, as in Fig. 3*b*, travel away from both sides of the switch, the value of the steps being

$$i_1 = i_2 = -I, \tag{7}$$

superposed upon the initial current I.

Now the voltage associated with the current in every travelling wave is given by the product of the current and the surge impedance Z of the line, with positive sign for waves

travelling forward and with negative sign for waves travelling backward, according to Fig. 3. We obtain therefore as voltages on the lines, immediately after the interruption,

$$\left.\begin{aligned} e_1 &= -Z_1 i_1 = Z_1 I \\ e_2 &= Z_2 i_2 = -Z_2 I, \end{aligned}\right\} \tag{8}$$

superposed upon the initial voltage E. In Fig. 3*b* the resultant distribution of the voltage is shown and we see that the circuit breaker voltage is

$$e_s = e_1 - e_2 = (Z_1 + Z_2)I. \tag{9}$$

It depends only on the current and the sum of the surge impedances. This is the total interrupting voltage, which produces travelling waves and oscillations within any winding. It divides on both sides of the circuit breaker according to equation (8) as

$$\frac{e_1}{e_s} = \frac{Z_1}{Z_1 + Z_2}; \qquad \frac{e_2}{e_s} = -\frac{Z_2}{Z_1 + Z_2}. \tag{10}$$

The subdivision thus depends only on the surge impedances of the lines or windings in the neighborhood of the switch. We can easily verify the initial distribution of voltages in Figs. 1 and 2, independently of the sign, if we consider that in Fig. 1 we have $Z_1 = Z_2$ and in Fig. 2 for the earth side, $Z_1 = 0$.

4. THREE-PHASE WINDING WITH STAR CONNECTION.

If we interrupt the first phase of a short-circuited star-connected winding as in Fig. 4, we can rearrange the parts of the winding adjacent to the circuit breaker as in Fig. 5, in order to get a diagram similar to Fig. 3. We realize that one side of the switch is connected to $Z_1 = Z$, the surge impedance of each phase winding, while the other side is connected to $Z_2 = Z/2$, the surge impedance of two phase windings in parallel. We therefore obtain the surge voltages

$$\frac{e_1}{e_s} = \frac{Z}{Z + Z/2} = \frac{2}{3}; \qquad \frac{e_2}{e_s} = -\frac{Z/2}{Z + Z/2} = -\frac{1}{3}. \tag{11}$$

The initial waves, which travel from both sides of the breaker, are therefore in the ratio of $-1:2$, as shown graphically in Fig. 5.

These waves travel through the various phase windings, all of the same length a, reach the star point exactly at the same time and there reunite. The phenomena in the neighborhood of the star point are shown in Fig. 6. The incident

FIG. 4.

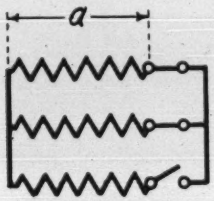

Interruption of the first pole of a star-connected three-phase winding in insulated state.

FIG. 5.

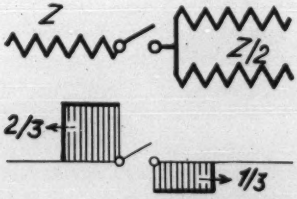

Development of interruption voltage in the case of Fig. 4.

waves are represented in Fig. 6*a*. Fig. 6*b* shows the refraction of the left-hand wave, which splits on passing the star point into two branches, each having 2/3 of the incident voltage. Simultaneously, a wave of 1/3 of the incident voltage is reflected. The right-hand waves, on the other hand, increase their voltage on passing the star point by uniting to 4/3 of the initial value. Fig. 6*c* shows the refracted wave and also the reflected wave of 1/3 of the incident voltage. These numerical laws of reflection and refraction are well known.

In Fig. 6*d* both waves are superposed. The voltage at the star point remains at zero, because both refracted waves of Fig. 6*b* and *c* have equal but opposite values. As a result there remain only discharge voltage waves on each side of the star point and these waves have the same value as the original

FIG. 6.

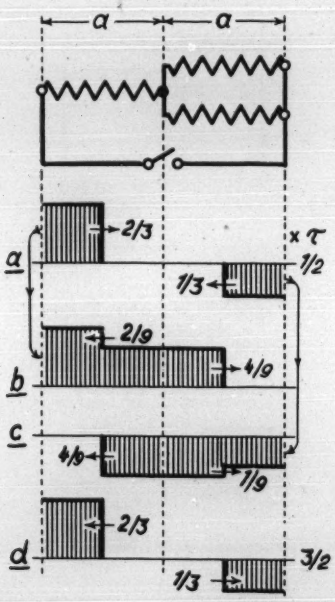

Interruption-voltage waves passing the neutral point in the case of Fig. 4.

incident waves. With this distribution of voltages the star point acts exactly like the center point in Fig. 1 or the left-hand short-circuit point in Fig. 2. The effect of two phase windings being in parallel thus consists in this case merely in an unequal subdivision of voltage. But this being without influence on the duration and travelling distance of the waves,

the natural frequency of each of the three-phase windings is given by

$$f_{Y1} = \frac{v}{4a}. \qquad (12)$$

FIG. 7.

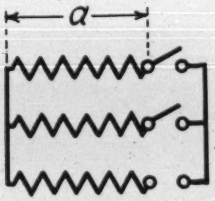

Interruption of the last poles of a star-connected three-phase winding in insulated state

FIG. 8.

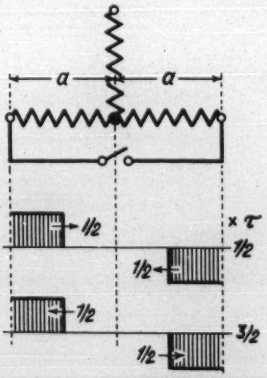

Voltage waves developed and passing the neutral point in the case of Fig. 7.

The interruption of the last phase of the star-connected winding is shown in Fig. 7. Here the subdivision of voltage at the breaker is $1/2 : -1/2$, the third pole being inactive. Fig. 8 shows the spatial behavior of waves in this case, which

is identical with that of Fig. 1 but with a different distance of travel. The star point remains unaffected, its voltage always being zero, and thus the third phase winding does not receive any voltage. It is wholly inactive in this case. As the incident waves are reflected at the star point with change of sign, this point acts as a short circuit point for the waves, although actually it is not grounded. Thus the natural frequency is

$$f_{v2} = \frac{v}{4a}, \tag{13}$$

We see, therefore, that for star-connected windings the interruption of the first phase as well as of the last phase excites the same natural frequency, determined by a travelling distance $4a$ of the waves and expressed by equations (12) and (13).

5. THREE-PHASE WINDING WITH DELTA CONNECTION.

The interruption of the first pole of a short-circuited delta-connected winding is shown in Fig. 9. We can rearrange the windings giving the linear diagram of Fig. 10 if we con-

FIG. 9.

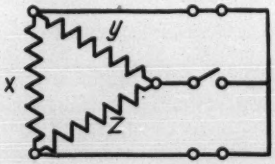

Interruption of the first pole of a delta-connected three-phase winding in insulated state.

sider that one pole of the interrupter is connected to two ends of the windings, the other pole to four ends of the windings, all being free from ground and able to float. While the phases y and z are in parallel and connected at both ends through the switch, the phase x is connected at both its ends to the same pole of the interrupting switch. Therefore we have drawn x in parallel halves in Fig. 10 so that the waves enter both ends with the same sign. The center of this third

phase, forming the left end of Fig. 10, is naturally quite free and can float also.

We see that in this case we have two lines of winding, both of length $1.5a$, connected at three points with each other, which must oscillate completely in parallel and in synchronism as if they were only one line of length $1.5a$ with open ends. This is indicated at the bottom of Fig. 10. As the travelling distance of any wave in this structure until its repetition is $3a$, the natural frequency for the delta winding is

$$f_{\Delta 1} = \frac{v}{3a}. \tag{14}$$

FIG. 10.

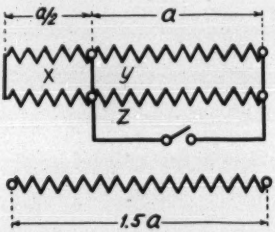

Straight-line diagram of the case of Fig. 9.

To clarify the performance of the switching waves further, Fig. 11 shows their distribution over the winding at a number of successive times until the distribution repeats. As one pole of the circuit breaker is connected to two ends and the other pole to four ends of the winding, the subdivision of the breaker voltage is $2/3 : 1/3$, exactly as in Fig. 5 and equation (11). The larger impulse impinges at the end of the winding, the smaller impulse impinges at $2/3$ of the resultant length. After the opening of the breaker and the creation of the incident waves, the entire winding is completely free from any external influence because the connecting cables to the breaker have only a negligible capacitance according to the assumptions made in the introduction. We see from Fig. 11 that the initial state is repeated after three periods τ of every

impulse travelling over one phase length, as given by equation (14). The fact that the exciting points for the travelling waves in this case are not at both ends of the resultant line does not alter in the least the natural frequency, though it

FIG. 11.

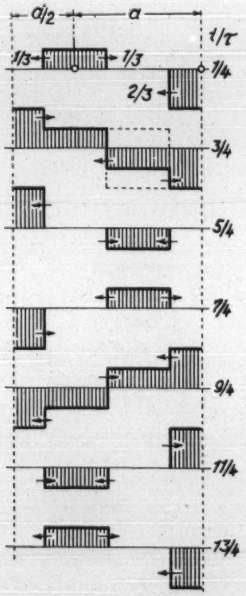

Voltage waves developed in the case of Figs. 9 and 10.

may influence the higher harmonics insofar as some of these may not be excited.

If we now interrupt the last two phases of the delta winding according to Fig. 12, we have symmetry of both terminals of the circuit breaker, so that half the interrupted voltage appears on each side. The incident waves pass into both adjacent phase windings, divide according to the arrows

in Fig. 12, and so we have four impulse waves which start to travel over the triangle. As the delta winding is absolutely free from any reflection or refraction points and forms a completely closed line, each of the four waves travels undisturbed through the whole winding of total length $3a$ until it comes back to the starting point. It repeats this journey again and again without ever changing its sign. As the period is 3τ, the natural frequency is

$$f_{\Delta 2} = \frac{v}{3a} . \qquad (15)$$

This is exactly the same value as for the first interrupted pole according to equation (14).

FIG. 12.

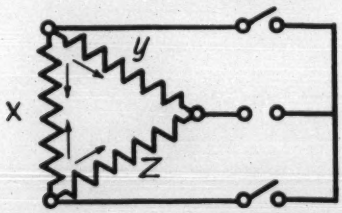

Interruption of the last poles of a delta-connected three-phase winding in insulated state.

In Fig. 13 the successive distributions of voltage over the delta winding are shown, the triangle being opened at one corner in order to draw it as a straight line. Thus the two end points are in reality connected together and do not form any reflection points. The various wave shapes are all formed by the superposition of the four voltage impulses incident at the junction of the two phases of the line, the last junction remaining free of incident voltage.

If we compare the natural frequencies of insulated star and delta connected windings according to equations (12/13) and (14/15), we see that they are in the ratio 4 : 3 and not $\sqrt{3}$: 1, as one perhaps might think at first sight.

FIG. 13.

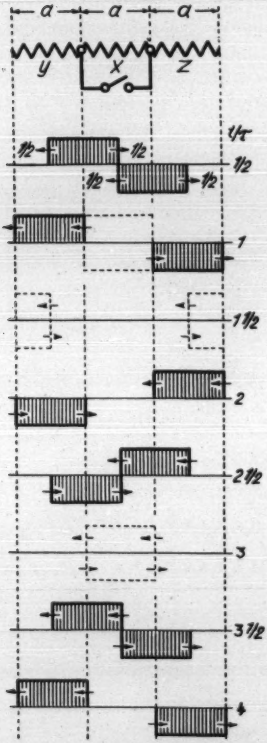

Voltage waves developed in the case of Fig. 12.

6. GROUNDED DELTA-CONNECTED WINDING.

As numerous short circuits in three-phase systems are formed by the action of already existing ground faults of one phase line, we will consider the interruption of short circuits while the system is grounded at one pole. As we measure all voltages between winding and ground, every ground

connection acts on the travelling waves as a short circuit point at which no voltage can exist.

The performance of star-connected windings under grounded conditions is rather complicated, and as that of delta windings is much simpler, we will consider them first.

The diagram of the interruption of the first pole of a grounded delta winding is shown in Fig. 14, this pole becoming

FIG. 14.

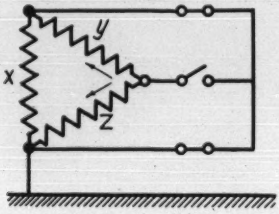

Interruption of the first pole of a delta-connected winding in grounded state, this pole belonging to the sound lines.

FIG. 15.

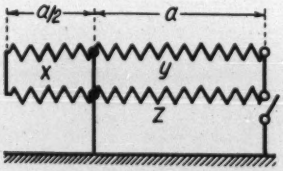

Straight-line diagram of the case of Fig. 14.

completely insulated. As the other two phases remain connected with ground, we can replace Fig. 14 by the straight line diagram of Fig. 15, which has exactly the same connections. It is similar to that of Fig. 10, except that now the common point of the three-phase windings is grounded. In consequence the third phase on the left-hand side, which was important in its action in Fig. 10, is excluded from any action in Fig. 15. It remains dead because no voltage can penetrate through a short-circuit point. Thus we have here exactly the same conditions as in Fig. 2, the fact that two windings are in parallel causing no change. The natural frequency of

the grounded delta winding for the first interrupting pole which is not connected to ground is therefore

$$f_{\Delta 1}' = \frac{v}{4a}. \tag{16}$$

This is different from the frequency in the ungrounded condition.

The interruption of the last poles of the same breaker is represented in Fig. 16. As the connecting point to ground acts as a short-circuit point, the entire interrupting voltage appears at the other end of the breaker. From its point of connection with the winding, voltage waves travel into both phase windings x and y. They are reflected at the grounded

FIG. 16.

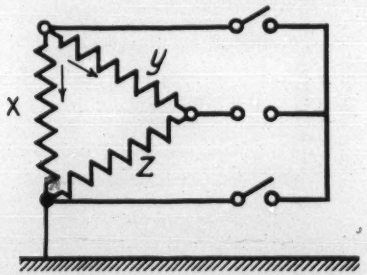

Interruption of the last poles of a delta-connected winding in grounded state, these poles being adjacent to the ground connection.

point with change of sign, the one after travelling a distance a, the other after a distance $2a$. If these waves return, they travel over the connecting point with the breaker without any distortion until they reach the other end of the winding, where again they are reflected with change of sign. Both waves therefore travel over a winding length $3a$ to and fro, and thus repeat their initial performance after travelling a distance $6a$. The natural frequency for this case is, therefore,

$$f_{\Delta 2}' = \frac{v}{6a}, \tag{17}$$

this being the frequency of a line of length $3a$ with both ends short-circuited to ground.

The full course of the voltage waves over the line is shown in Fig. 17 for successive instants of time. The winding is fed

FIG. 17.

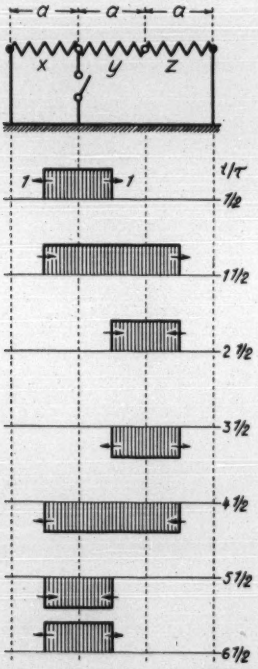

Development of voltage waves in the case of Fig. 16.

at one-third of its length by the initial waves, which spread to both sides. By the reflection with change of sign at the ends the whole voltage is concentrated after a time 3τ at the other phase junction, then it spreads again over the winding,

and after 6τ the waves concentrate again at the initial exciting point.

In Figs. 14 and 16 we have treated the case where one of the sound or insulated poles is interrupted first, and the last interruption takes place at the pole with the ground fault. However, the opposite sequence has the same probability and Fig. 18 shows the diagram for this condition with interruption of the grounded pole first, while the two sound poles remain connected to each other. Here the full voltage appears at both of these sound poles and four partial waves travel over the windings. By comparison with Fig. 16 we see that each of the two sound poles of this case acts exactly

FIG. 18.

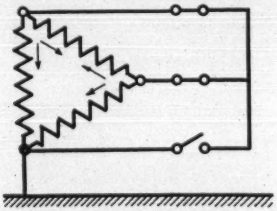

Interruption of the first pole of a delta-connected winding in grounded state, this pole being adjacent to the ground connection.

like the last sound pole treated in Fig. 16. We have here therefore simply a doubling of all travelling waves by feeding both free poles or phase junctions instead of one only, as shown in Fig. 17. Without drawing the whole combined diagram we see that the travelling distances and therefore the repetition periods are not altered. The natural frequency if the ground fault pole is interrupted first is therefore

$$f_{\Delta 1}'' = \frac{v}{6a}. \qquad (18)$$

Figure 19 shows the interruption of the last poles in this case. As both are insulated and symmetrical after the interruption, the corresponding phase junctions receive equal but opposite interruption voltage, $\pm 1/2$ the total value.

Both voltages spread over the windings in four waves similar to Fig. 18, only with different magnitudes and signs. However, these waves now being opposite each other, the halves of the complete delta winding act one against the other. We see this immediately if we impress $\pm E/2$ on the two-phase junctions in Fig. 17, which gives exactly the same course of waves as in Fig. 13. The center of this diagram is now a point of symmetry between opposite halves and acts therefore like a short-circuit point. Thus we obtain for each

FIG. 19.

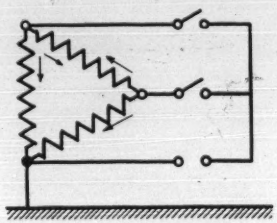

Interruption of the last poles of a delta-connected winding in grounded state, these poles belonging to the sound lines.

half winding and therefore also for the complete delta winding a natural frequency

$$f_{\Delta 2}'' = \frac{v}{3a}. \qquad (19)$$

We have seen in Parts 4 and 5 that the natural frequencies of insulated or ungrounded three-phase windings remain the same for the first and last interrupting pole of the circuit breaker, this being valid for star connection as well as for delta connection. From equations (16) to (19) we realize that in a grounded system it is merely a matter of chance whether the first or the last excited frequency is the higher, both always being different. Because we cannot predict whether the first quenched arc in the circuit breaker belongs to the line with fault or to a sound line, the first frequency excited may vary as 3 : 2, the last one as 1 : 2, three of these possible frequencies always being different from the frequency for the insulated state of the entire winding.

(To be continued.)

NOTES FROM THE NATIONAL BUREAU OF STANDARDS.*

DAYTIME PHOTOELECTRIC MEASUREMENT OF CLOUD HEIGHTS.

"Ceiling-zero" is one of the most dangerous hazards to aviation. The height of the ceiling and information concerning the rate at which it is rising or falling above an airport are of particular interest to the pilot who is scheduled to land there within an hour or so. In the United States and Canada, the meteorological services use "ceiling projectors" to determine the height of clouds at night. An intense beam of light from a projector forms a very conspicuous spot on the base of the cloud directly above it. An optical instrument is used to measure the angle between the line of sight on the spot and the line of sight on the projector. This angle of elevation of the spot, together with the known distance between the optical instrument and the projector, permits the calculation of the height of the cloud ceiling by simple trigonometry.

During the daytime, however, the clouds are so bright that the spot is not visible and hence the usual optical instrument cannot be used to measure the angle required to make the calculation. Modulating the beam from the projector, that is, breaking it up into short evenly spaced pulses of light, has made it possible to detect the reflected signal light with a photoelectric tube and amplifier. These were designed to respond only to that component of the total light received from the clouds which has the characteristic pulses introduced into the projected beam. Thus, the projected signal light, after reflection, is sorted out from the background light of the cloud. In use the photoelectric detector scans the base of the cloud until the meter on the amplifier indicates that the modulated signal light is being received. The angular setting of the detector then corresponds to the angular elevation of the spot on the cloud. Two members of the Bureau's Electricity Division, Maurice K. Laufer and Laurence W.

* Communicated by the Director.

Foskett, have developed this equipment for the U. S. Weather Bureau, and the project was financed by that agency. During the daytime, cloud ceilings as high as 9,000 feet have been detected.

MAGNETIC SATURATION INDUCTION OF IRON.

The magnetic saturation induction of a ferromagnetic material is the limit of the intrinsic magnetization theoretically possible by the application of a magnetizing force of infinite intensity. The value is of interest primarily from the point of view of the theory of ferromagnetism. One of the principal obstacles heretofore encountered in the determination of the saturation value of iron has been the difficulty of obtaining iron of a sufficiently high degree of purity. It has also been hard to obtain a satisfactory degree of accuracy in the magnetic measurements.

Several ingots of exceptionally pure iron have recently been prepared at the Bureau. The total amount of the impurities determined by the best available methods of analysis is of the order of 0.01 per cent. R. L. Sanford and E. G. Bennett have made magnetic measurements on several specimens from these ingots, and special precautions have been taken to obtain the highest possible accuracy.

In a report (RP1354) in the January *Journal of Research*, the methods by which the measurements were made are described. The value reported for the magnetic saturation induction of pure iron at 25° C. is 21.58 ± .01 kilogauss.

THERMAL EXPANSION OF ELECTROLYTIC CHROMIUM.

An investigation of the linear thermal expansion of electrolytic chromium has recently been completed by Peter Hidnert. A total of 15 tests were made on two samples (99.3 and 98.7 per cent. chromium) at various temperatures between −105° and +715° C. with a precision comparator method and with an interference method.

During the first heating or heatings, when hydrogen presumably was being evolved, the samples contracted in an

irregular manner. After a few heatings, however, the irregularities disappeared and smooth expansion curves were obtained.

After the first heating to 500° C. and cooling to room temperature, the 99.3 per cent. sample was 1.1 per cent. shorter than the initial length before heating. The density of this sample increased 2.4 per cent. and the volume decreased 2.3 per cent., after three cycles of heating to 500° C. and cooling to room temperature.

The linear thermal expansion of electrolytic chromium is a function of the temperature, hydrogen content or liberation, time and rate of heating, previous treatment, etc. during the first heating or when irregularities (contraction) occur.

Equations for calculating the instantaneous coefficient of expansion and the length at any temperature between −100° and +700° C., and other details of the work will be found in RP1361 in the *Journal of Research* for January. The following table gives average calculated coefficients of expansion:

Temperature Range.	Average Coefficient of Expansion per Degree Centigrade.
° C.	$\times 10^{-6}$
−100 to 0	5.1
0 to 100	6.6
0 to 200	7.3
0 to 300	7.9
0 to 400	8.4
0 to 500	8.8
0 to 600	9.1
0 to 700	9.4

HYDROLYSIS OF TURANOSE.

Turanose (3-α-*d*-glucopyranosido-*d*-fructose) differs from the more common disaccharides in that the glycosidic union is on the carbon adjacent to the reducing group. The proximity of the reducing group influences the stability of the glycosidic union and causes the disaccharide to be particularly susceptible to alkaline hydrolysis. On treatment with lime water, turanose undergoes hydrolysis rather than a normal Lobry de Bruyn interconversion. In the presence of oxygen, in alkaline solution, the sugar is hydrolyzed in large measure and the resulting glucose and fructose are oxidized to arabonic

acid. On the other hand, lactulose (4-β-*d*-galactopyranosido-*d*-fructose) is relatively stable to alkaline hydrolysis, and when treated with oxygen in solution containing potassium hydroxide it yields the salt of a disaccharide acid, presumably 3-β-*d*-galactopyranosido-*d*-arabonic acid. The difference in the behavior of the two sugars illustrates the importance of the location of the glycosidic union in relation to the behavior of the sugars in alkaline solution. The location of the glycosidic union also affects the amount of reduction with alkaline copper reagents. In the January *Journal of Research* (RP1356) Horace S. Isbell reports copper reducing values for turanose at several concentrations, as obtained by the Munson-Walker method.

SURFACE CHARACTERISTICS OF COTTON FIBERS.

Natural cotton is composed of a primary and a secondary wall. The former forms a thin sheath on the surface of the fiber and is composed principally of small amounts of cellulose embedded in a membrane of wax and pectic substance. The latter is composed chiefly of cellulose and forms the main body of the fiber. The pectic substance, although present to the extent of only approximately 1 per cent., accounts for 85 per cent. of the total acidic groups of the mature fiber. The highly acidic nature and the location of this substance in the naturally occurring fibers would be expected to influence greatly a number of the properties of the fibers, especially those dependent on surface characteristics. These surface characteristics are of considerable importance in a number of industrial processes such as, for example, the scouring, dyeing, and finishing of textile materials.

Since the electrophoretic technique has been shown by research associates for the Textile Foundation at the Bureau to be a useful tool for characterizing other fiber surfaces, it appeared advisable to apply it to an investigation of the cotton fiber as well. As shown in a report by Arnold M. Sookne and Milton Harris (RP1359 in the January *Journal of Research*), samples of dewaxed cotton, cotton which had been depectinized by treatment with a boiling 1-per cent. solution of sodium hydroxide for various lengths of time, and pectic substance

from cotton gave widely different pH-mobility curves. The curve for pectic substance is characteristic of a highly acidic substance whereas that of depectinized cotton appears to be a composite of the curves for cellulose and pectic substance.

The purified cellulose exhibits a reversal of charge below pH 2.5, and accordingly is isoelectric at that pH. It is shown that the reversal of charge has not resulted from irreversible changes produced in the fiber during immersion in the dilute solutions of acid used in the present investigation.

COMBINATION OF SILK FIBROIN WITH ACID AND WITH BASE.

Silk contains a number of acidic and basic groups. Their state of combination and behavior is important in influencing the tensile and elastic properties of the fibroin and the adsorption of moisture and dyes.

As part of the program of the Textile Foundation Research Associateship at the Bureau, the relationship between the quantities of hydrochloric acid and potassium hydroxide taken up by fibroin from solutions and the concentrations of those solutions, were investigated. The effect of added potassium chloride was also studied. In general, it has been possible to correlate the several parts of the titration curves of proteins with their amino acid contents, but knowledge of the role of the phenolic hydroxyl groups of tyrosine has always been limited. Silk fibroin, however, contains such a large proportion of tyrosine as practically to assure an indication of the role of the phenolic hydroxyl groups of tyrosine simply by the magnitude of the base-binding capacity. In order to investigate more carefully the part taken by these groups, Leland F. Gleysteen and Milton Harris have obtained a titration curve for methylated fibroin in which most of the hydroxyl groups have been converted into nonreactive methoxyl groups.

The component parts of the titration curve of silk fibroin have been interpreted in terms of the composition of this protein. Thus, the hydroxyl groups of tyrosine appear to bind base as shown by the fact that the base-combining capacity is much greater than can be accounted for by the other groups which are able to bind base.

The presence of free carboxyl groups in silk fibroin is suggested by the shape of the titration curve. From the maximum amount of acid bound an estimate of the total content of free amino groups may be obtained. The effect of added salt is similar to that obtained with other insoluble proteins, namely to increase the quantity of acid or base bound at a given pH, in a manner which suggests that the combination of hydrogen ions is affected by the concentration of anions as well as by the concentration of hydrogen ions and that combination with hydroxyl ions is affected by the concentration of cations.

A complete account of this work will appear in the January *Journal of Research* as RP 1360.

PAINTS FOR EXTERIOR MASONRY.

Special paints are often used on exterior walls of porous masonry to keep out moisture and to give them an attractive finish. The Bureau is studying the behavior of these masonry paints, as part of the general research program on construction materials and methods for low-cost housing. To facilitate the work, a test field has been built where masonry paints can be applied under practical working conditions, after which a careful watch can be kept to determine the effects of exposure.

The materials used in constructing the test walls include new and used common brick, cinder block, expanded blast furnace slag block ("Pottsco"), concrete block, cast-in-place concrete, and cement-asbestos siding. The walls are vertical and face north and south. The painting surface of the walls is from 11 to 11.5 square feet, with the exception of the ones on which cement-asbestos siding was used; these measure approximately 32 square feet.

Commercial brands of oil and varnish paint, emulsified synthetic resin paints, chlorinated rubber coatings, rubber emulsion paints, and cement-water paints have been applied to each type of test surface. The use of cement-sand grout coat as a base on open joint and extremely porous walls and the efficiency of rubber primers on "green" walls are being

given particular attention in the painting procedures and in the study of the compatibility of dissimilar paint coatings.

The hiding power and color of the paints were determined by instruments at the time of painting, and changes in these properties are being followed by monthly measurements made with a portable reflectometer. The spreading rate, brushing properties, drying characteristics and recoatability were also recorded for each paint on each type of surface. The relative moisture content of the walls at the time of painting and from time to time afterwards is determined with a "moisture meter."

In addition to the 193 test walls now undergoing exposure, a small house (10 × 12 feet) with single walls of 8- × 8- × 16-inch 3-cell cinder block and an exposed chimney of common brick is being used for further study of masonry coatings under service conditions.

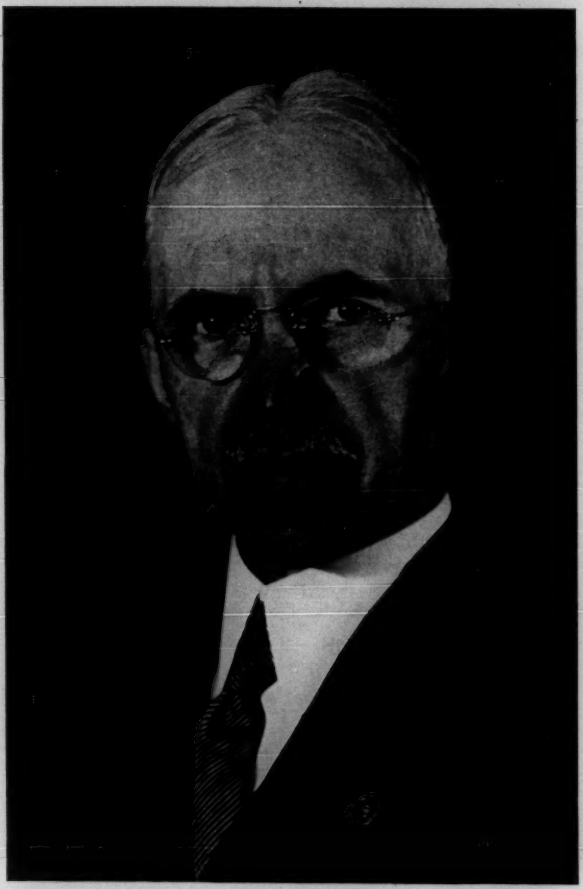

ALFRED RIGLING, M.A.

LIBRARIAN

ASSISTANT SECRETARY ASSISTANT EDITOR

1883–1940

THE FRANKLIN INSTITUTE.

ALFRED RIGLING,

1868–1940.

"It is with profound sorrow that the Board of Managers of The Franklin Institute records the death of ALFRED RIGLING, Honorary Master of Arts of the University of Pennsylvania, for fifty-eight years Librarian of The Franklin Institute, and for thirty-two years Assistant Secretary and Assistant Editor of the JOURNAL. Mr. Rigling departed this life on December eighth, nineteen hundred and forty.

"A quiet and unassuming gentleman, Mr. Rigling served for fifty-eight years the Society which he loved with unswerving devotion, keeping in touch with its progress and growth, expanding himself to keep abreast of the times—with this one object in view—to better serve The Franklin Institute.

"Alfred Rigling was born and educated in Philadelphia. He came to work in the Institute when fourteen years old. At the age of nineteen he was made Librarian, when the Library contained some eighteen thousand volumes. He watched and guided its growth to its present size and distinction, and was content when its fame as a patent and technical library spread throughout the world.

"In 1908 he was elected Assistant Secretary of The Franklin Institute and was called upon to perform the duties of Secretary, as in times of illness and during the World War—and always he performed them well. As Assistant Editor of the JOURNAL of the Institute his services were invaluable, as for many years he took charge of the mechanical operations connected with its publication.

"The Franklin Institute was proud of the outstanding service rendered by Mr. Rigling, and in 1933, upon the occasion of his fiftieth anniversary of service, conferred upon him Honorary Membership 'in recognition of a half century of helpful and intelligent service, during which long term of duty well done he has been a pillar of strength to the Institute, a source of comfort to the discouraged and of knowledge to the ignorant: a librarian amazingly informed concerning his library, and a kindly gentleman—skillful and eager in friendly service to his fellow-men.' The sentiments persisted and increased until the time of his death.

"Here is recorded the death of a devoted and trusted servant, who was the very embodiment of the spirit of The Franklin Institute—an esteemed friend, a trusted adviser, an untiring worker. We are poorer for his passing.

"*Therefore be it resolved:* That this Minute be entered upon the Records of the Board, and that an appropriate announcement be published in the JOURNAL OF THE FRANKLIN INSTITUTE:

"*Be it further resolved:* That a copy of this Minute be sent to Mrs. Rigling, with expressions of deepest sympathy from the members of the Board of Managers of The Franklin Institute.

January 15, 1941

EDWARD G. BUDD,
G. H. CLAMER,
MAX TRUMPER."

Not only in The Franklin Institute was Mr. Rigling esteemed. In 1933 the University of Pennsylvania bestowed upon him an Honorary Master of Arts Degree.

He was held in affectionate regard by other librarians throughout the City and State. He served as Chairman of the Special Libraries Council of Philadelphia from 1931 to 1935 and was publicly honored by his associates upon his fiftieth anniversary with the Institute.

In 1935 he was elected a Fellow of the American Association for the Advancement of Science.

In the interest of The Franklin Institute, Mr. Rigling devoted much time and energy to the Alumni Association of the Schools of the Institute which were discontinued in 1923. He was for twenty-five years secretary of the Alumni Association, keeping its members in touch with affairs of the Institute, seeking out men whom he knew had received their early training in the schools, and in many ways sustaining this Association, important to the Institute.

ANNUAL MEETING, JANUARY 15, 1941.

The annual meeting of The Franklin Institute was held on the evening of Wednesday, January 15, 1941, at 8:15 o'clock, with Mr. Philip C. Staples, President, presiding.

The minutes of the previous meeting were approved as published in the January issue of the JOURNAL.

The Chairman called upon the Secretary, Dr. Henry Butler Allen, who read the report of the Tellers of the annual election; whereupon the following gentlemen were declared elected to the respective offices:

President (to serve one year)	Philip C. Staples
Vice-Presidents (to serve one year)	Walton Forstall
	W. Chattin Wetherill
	S. S. Fels
	Richard W. Lloyd
Treasurer (to serve one year)	M. M. Price
Managers (to serve three years)	G. H. Clamer
	Clarence L. Jordan
	Leonard H. Kinnard
	Conrad N. Lauer
	Lionel F. Levy
	Richard T. Nalle
	Charles Penrose
	Philip H. Ward, Jr.
(to serve two years)	Edward Warwick
(to serve one year)	Charles S. Redding

The additions to membership since the last report were as follows:

Active	7
Associate	10
Student	51
Total	68

The Chairman presented the Annual Report of the Board of Managers on the activities of the Institute during the year 1940.

The Chairman then introduced the speaker of the evening, The Honorable G. Grant Mason, Jr., Member, Civil Aeronautics Board, Washington, D. C., who addressed the meeting on "American Civil Aviation Today as a Decisive Factor in World Affairs."

The speaker, a noted figure in aviation circles, was appointed by the President as one of the five Members of the new Civil Aeronautics Authority in 1938. He was appointed by that body to make a survey of European civil aviation on behalf of the United States Government in September and October of the same year, and since July, 1940, he has been a Member of the Civil Aeronautics Board.

In introducing his topic Mr. Mason stated that he would present a review of the past development of aviation, a study of current trends, and some suggestions as to its future. He pointed out, in his discourse, that aviation has revolutionized methods of aggression and warfare, that the United States must take stock of its own aeronautical resources, and that American civil aviation today is a potentially decisive factor in national and hemisphere defense, as well as in world affairs. His paper in full will appear in a later issue of this JOURNAL.

The meeting was dismissed with a rising vote of thanks to the speaker of the evening.

HENRY BUTLER ALLEN,
Secretary.

COMMITTEE ON SCIENCE AND THE ARTS.

(Abstract of Proceedings of Stated Meeting held Wednesday, January 8, 1941.)

HALL OF THE COMMITTEE,
PHILADELPHIA, JANUARY 8, 1941.

DR. FREDERIC PALMER, JR., *in the Chair.*

The following report was presented for final action:

No. 3087 / No. 3088 The Standing Sub-Committee on the Franklin Medal recommended that a Franklin Medal be awarded in 1941 to:—

EDWIN HOWARD ARMSTRONG, of New York City, New York, "In recognition of his pioneer work in regeneration and the oscillating vacuum tube circuits, in the invention of the superheterodyne circuit, the super-regenerator, and a system of wide-swing frequency modulation, each an outstanding contribution to the communication art"; and one to

CHANDRASEKHARA VENKATA RAMAN, of Bangalore, Mysore, India, "In recognition of his many brilliant contributions to physical science and of his leadership in the renaissance of scientific work and scientific education that has occurred in India during the last thirty years."

JOHN FRAZER,
Secretary to Committee.

LIBRARY NOTES.

Photostat Service. Photostat prints of any material in the collections can be supplied on request. Orders received in the morning are filled the same day. The average cost for a print $8\frac{1}{2} \times 11$ inches is forty cents.

The library and reading room are open on Mondays, Tuesdays, Fridays and Saturdays from nine o'clock A.M. until five o'clock P.M., Wednesdays and Thursdays two until ten o'clock P.M.

RECENT ADDITIONS.

AGRICULTURE.

PARRISH, P., AND A. OGILVIE. Calcium Superphosphate and Compound Fertilisers. 1939.

ARCHITECTURE AND BUILDING.

American Concrete Institute. Proceedings. Volume 36. 1940.

ASTRONOMY.

NININGER, H. H. Our Stone-Pelted Planet. 1933.

BIOLOGY AND BIOCHEMISTRY.

LUYET, B. J., AND P. M. GEHENIO. Life and Death at Low Temperatures. 1940.

CHEMISTRY AND CHEMICAL TECHNOLOGY.

CURTMAN, LOUIS J., AND SYLVAN M. EDMONDS. Calculations of Qualitative Analysis. 1940.

MCKAY, H., AND H. A. C. MCKAY. The Ideas of Physical Chemistry. 1934.

NEWITT, D. M., Editor. Chemical Industries. No Date.

RHODES, HENRY T. F. Forensic Chemistry. 1940.

SAND, HENRY J. S. Electrochemistry and Electrochemical Analysis. Two volumes. 1939–1940.

TIMMERMANS, JEAN. Chemical Species. Translated from the Revised French Manuscript by Ralph E. Oesper. 1940.

VILBRANDT, FRANK C. Chemical Engineering Plant Design. First Edition. 1934. Chemical Engineering Series.

ELECTRICITY AND ELECTRICAL ENGINEERING.

BUTLER, J. A. V. Electrocapillarity. 1940.

FRANK, NATHANIEL H. Introduction to Electricity and Optics. First Edition. 1940.

Radio Handbook, by the Editors of "Radio." Seventh Edition. 1940.

U. S. Federal Power Commission. Directory of Electric Utilities in the United States. 1940.

ENGINEERING.

American Society for Testing Materials. 1940 Supplement to A. S. T. M. Standards. Parts 1–3. 1940.

HUDSON, J. C. The Corrosion of Iron and Steel. 1940.

TIMOSHENKO, S. Strength of Materials. Part 1. Second Edition. 1940.

GEOLOGY AND GEOPHYSICS.

American Institute of Mining and Metallurgical Engineers. Transactions. Geophysics. 1940.

MANUFACTURES.

SKINKLE, JOHN H. Textile Testing. 1940.

MECHANICAL ENGINEERING.

GIESECKE, FREDERICK E., ALVA MITCHELL, AND HENRY CECIL SPENCER. Technical Drawing. Second Edition. 1940.

SMITH, ROBERT H. Text-book of Advanced Machine Work. Twelfth Edition, Revised and Enlarged. 1940.

MINING AND METALLURGY.

ADDICKS, LAWRENCE, Editor. Silver in Industry. 1940.

American Society for Metals. Age Hardening of Metals. 1940.

BUGBEE, EDWARD E. A Textbook of Fire Assaying. Third Edition. 1940.

McGraw-Hill Publishing Company. Metal and Non-Metallic Mining Catalogs. Eighteenth Edition. 1940.

NAVAL ARCHITECTURE AND NAVIGATION.

CLOWES, G. S. LAIRD. The Story of Sail. 1936.

MCKAY, LAUCHLAN. The Practical Shipbuilder. Published in Original Format. 1940.

MIXTER, GEORGE W. Primer of Navigation. 1940.

PATENTS.

THOMAS, EDWARD. Handbook of Chemical Patents. 1940.

PHOTOGRAPHY.

BOUCHER, PAUL E. Fundamentals of Photography. 1940.

U. S. Camera 1941. Two volumes. 1940.

PHYSICS.

DEN HARTOG, J. P. Mechanical Vibrations. Second Edition. 1940.

SUGAR.

BASSETT, SARA WARE. The Story of Sugar. 1926.

NOTES FROM THE BARTOL RESEARCH FOUNDATION.

COMPARATIVE EFFICIENCIES OF RADIOACTIVE NEUTRON SOURCES.*

BY

S. A. KORFF, E. T. CLARKE, E. J. MURPHY,† W. C. BRIGHT † and M. D. WHITAKER.†

We have measured the comparative neutron-producing efficiencies of several radium-beryllium and radon-beryllium neutron sources in order to determine whether these efficiencies are proportional to the gamma-ray activities of the sources. Neutron production from such sources has been customarily assumed proportional to the gamma-ray intensity, and furthermore it has been stated that radon-beryllium sources are more efficient than radium-beryllium sources.

Four radium-beryllium and two radon-beryllium sources were compared by placing the sources successively in a paraffin block, near which was located a boron-trifluoride-filled detecting chamber connected to a linear amplifier. Care was taken that the geometry should be the same in each measurement. The counting rate of the chamber, with and without a half-millimeter-thick cadmium shield, gave a measure of the slow neutron intensity. By establishing that there was no observable change in counting rate when 200 milligrams of radium without beryllium were brought up, it was ascertained that the strong gamma-ray intensity from these sources did not influence the detecting efficiency. The gamma-ray strengths of the several sources had been previously determined by standard procedures.

Table I shows the relative neutron yield per milligram-equivalent for the various sources. It will be observed that the yield is different for each of the five sources, and further-

* Reprinted from *The Physical Review*, 58, 88 (1940).

† New York University, University Heights, New York, N. Y.

TABLE I.

Observed Yields of Neutrons per Millicurie of Gamma-ray Activity in the Source.

Type.	Approximate Strength (Gamma-Ray).	Neutrons/mg.-Equiv. (Relative).
Ra-Be	200 mg.	1
Ra-Be	200 mg.	0.97
Ra-Be	200 mg.	0.85
Ra-Be	9.87 mg.	0.88
Rn-Be	60 mC.	0.55
Rn-Be	30 mC.	0.76

more that the radon sources are considerably less efficient than the radium-beryllium sources. It is therefore evident that serious error may be made by assuming the neutron yield to be proportional to the gamma-ray intensity. The beryllium content of the above sources varies between 0.1 gram and 5 grams, the large radium sources containing the greater quantities of beryllium. More details of these measurements and a discussion of the efficiency variations will be published in a forthcoming issue of the JOURNAL OF THE FRANKLIN INSTITUTE.

NOTES FROM THE BIOCHEMICAL RESEARCH FOUNDATION.

The Fractionation of Certain Pancreatic Extracts which Influence Fat Metabolism.—VINES COLLIER, JR. Pancreatic extracts influence fat metabolism, particularly in the liver (Dragstedt et al., *Amer. Jour. Physiol.*, **117**: 167, 175, 1936; Channon et al., *Biochem. J.*, **32**: 1332, 1938; McHenry and Gavin, *Jour. Biol. Chem.*, **134**: 683, 1940). Inasmuch as this lipotropic action cannot be explained on the basis of the choline, protein or enzyme content of such extracts, an attempt to isolate and identify other active constituents has been made.

Extracts of both fresh pancreas and the dried residue from the isolation of insulin have been prepared by Dragstedt's procedure and by a new method. In this new method the tissue was extracted with a concentration of alcohol equivalent to 60 per cent. and containing one cc. of concentrated hydrochloric acid per gallon. The extract was reduced in volume *in vacuo* at 50° C., the fats were removed by ether extraction or cooling followed by filtration. Treatment of the extract with a saturated aqueous solution of mercuric chloride gave a precipitate. This precipitate, freed of mercury with hydrogen sulfide, has been proved to be a mixture of the purine bases adenine and guanine, plus some highly-colored inactive material. The portion of the extract not precipitated by mercuric chloride has not yet been identified.

Subcutaneous administration of various extracts and fractions to over 600 mice, utilizing the seven-hour technic of Campbell (*Endocrinology*, **23**: 692, 1938), showed that the whole extracts caused an increase in the liver fat of both males and females. However, the purine fraction caused a decrease in the liver fat of males and an increase in that of females. The portion of the extract not precipitable with mercuric chloride produced an exactly opposite effect, causing an increase in the liver fat of males and a decrease in that of females.

The effects of the two fractions were tried on 143 rats on either normal or high fat diets. These animals were given subcutaneous injections of the fractions being tested, for periods of from three to fourteen weeks. Total fatty acids of liver and serum were determined by Bloor's method (*Jour. Biol. Chem.*, **77**: 53, 1928), and phospholipid by King's (*Biochem. J.*, **26**: 292, 1932) colorimetric method for phosphorus. The fatty acid content of the livers of rats on normal diets was not affected by either fraction. That of rats on high fat diets, however, was affected in exactly the same manner as was noted above for normal mice, i.e., the purine fraction caused a decrease in the fatty acid content of the livers of males and an increase in that of females, the mercury soluble fraction caused an increase in the fatty acid content of the livers of males and a decrease in that of females. The differences in the serum fatty acid content are not believed to be significant. The phospholipid content of both serum and liver was found to be very stable and was not influenced by either diet or treatment.

Dried brewers' yeast has been found (Hortenstine et al., *Jour. Biol. Chem.*, **125**: 455, 1938; McHenry and Gavin, *Jour. Biol. Chem.*, **134**: 683, 1940) to be effective in preventing fatty livers and our work suggests that this preventive action may be due to the purine content of the yeast. Further experiments on this subject and other experiments to determine the mode of action of these fractions of pancreatic extract on fat metabolism are now under way.

From these results it seems evident that there are at least two factors in pancreatic extracts which influence fat metabolism: one, a mixture of the purine bases, adenine and guanine, and possibly their higher derivatives, and the other as yet unidentified.

The Preparation of Some 2-Pyridyl and 8-Quinolyl Phenyl Sulfides and Sulfones.—HARRY C. WINTER AND FRANCIS E. REINHART (*Journal American Chemical Society*, **62**: 3508, 1940). The discovery of the powerful antistreptococcal properties of sulfanilamide, 4,4′-dinitrodiphenyl sulfone, and some of their derivatives has led to the investigation of a large number of related compounds of the benzene

series. Very little attention, however, has been directed to the pyridine and quinoline analogs of these active therapeutic agents. In fact, only two such compounds, 6-sulfonamidoquinoline and 2,2′-dipyridyl sulfide, had been studied when an investigation of these analogs was begun in this Laboratory. Recently, there has been reported the preparation of a number of sulfonamides, sulfides and sulfones of pyridine and quinoline. The value of these compounds as antistreptococcal agents has not yet been established.

The compounds prepared in this investigation have been chiefly 2-pyridyl or 8-quinolyl sulfides and sulfones in which a phenyl or *p*-nitrophenyl group was present as the second substituent. In all of these, a nitro or amino group occupied that position in the heterocyclic nucleus para to the sulfur linkage thus simulating the relative positions of these groups in the active antistreptococcal compounds of the benzene series.

The mononitro sulfides (5-nitro-2-pyridyl phenyl and 5-nitro-8-quinolyl phenyl) were made by condensing thiophenol with 2-chloro-5-nitropyridine or 5-nitro-8-chloroquinoline. The use of *p*-nitrothiophenol in place of thiophenol resulted in the formation of the expected dinitro sulfides containing a *p*-nitrophenyl group. When the mononitro sulfides were reduced with stannous chloride, the corresponding amino sulfides were obtained.

The oxidation of the nitro sulfides with 30 per cent. hydrogen peroxide or, in one case, with chromic acid, led to the formation of the corresponding sulfones. Although 5-amino-2-pyridyl phenyl sulfone was easily made by oxidation of the amino sulfide, 5-amino-8-quinolyl phenyl sulfone was best prepared by careful reduction of the corresponding nitro sulfone with the calculated quantity of stannous chloride. In addition, 5-nitro-2-pyridyl *m*-nitrophenyl sulfone resulted upon nitration of 5-nitro-2-pyridyl phenyl sulfone.

In connection with this work one other new compound, 8-quinolinesulfanilyl sulfanilic acid, and several known compounds were prepared for evaluation as antistreptococcal agents. These were potassium 5-nitro-2-pyridinesulfonate, 5-amino-2-pyridinesulfonic acid, 8-quinolinesulfonic acid, 8-quinolinesulfonamide, and 8-amino-5-quinolinesulfonic acid.

5,5′-Dinitro-2,2′-dipyridyl and 5,5′-dinitro-8,8′-diquinolyl sulfides were made as subsequently described by Surrey and Lindwall.

These known compounds as well as the mononitro sulfones, the amino sulfones, the amino sulfides, 5-nitro-2-pyridyl phenyl sulfide, and 8-quinolinesulfanilyl sulfanilic acid were found to be ineffective when tested in mice for antistreptococcal activity.

Systematic Qualitative Organic Microanalysis: Determination of Specific Gravity.—HERBERT K. ALBER (*Industrial and Engineering Chemistry*, Analytical Edition, **12**: 764, 1940). The general applicability of decigram, centigram, and milligram pipets has been demonstrated for the determination of specific gravities of liquids and solids. The accuracies obtainable under ordinary laboratory conditions are sufficiently high for a safe identification of unknown liquids or solid organic compounds in qualitative organic microanalysis, as shown by their satisfactory use over more than five years by different investigators.

The Determination of Average Molecular Weights or Particle Sizes for Polydispersed Systems.—ELMER O. KRAEMER (JOURNAL OF THE FRANKLIN INSTITUTE, **231**: 1, 1941). The significance of an average value of particle size or molecular weight for a polydispersed substance depends upon the relationship between particle size or molecular weight and the property used in determining the average value. If the entire distribution curve of the polydispersed substance is known, the meaning of an average value depends upon the manner in which the summations defining the average are carried out. A general equation is formulated, with the aid of which the significance of measurements of physical or chemical properties of polydispersed substances in terms of rational average values may be readily ascertained. The mode of procedure is illustrated in explicit fashion for the viscosity of spherical and ellipsoidal particles, light absorption and scattering, as well as ultracentrifugal measurements.

BOOK REVIEWS.

THE STORY OF SUPERFINISH, by Arthur M. Swigert, Jr. 672 pages, illustrations, plates, 16 × 24 cms. Detroit, Lynn Publishing Company.

Everyone versed in the mechanic arts knows the value of a smooth surface when that surface periodically or continually comes in contact with another smooth surface. The total machinery losses, in the United States alone, due to friction, if they were known, would reach a figure beyond belief. This fact has been recognized for many years and successful efforts have been made through the application of physics, metallurgy and engineering to reduce these losses by developing a smoother metal finish which when properly lubricated will result in less wear. Superfinish is a late development along these lines. It is the removal from the surface of a dimensionally finished metal part the fragmented metal resulting from turning, grinding, honing and lapping, when dimension and finish are simultaneously produced. Mechanically the surface is metallurgically changed from a fragmented surface of ruptured metal to a surface of smooth, unworked, crystalline metal capable of carrying greater bearing loads per unit area with either total or practically total wear elimination when properly lubricated. Yet there is removed from this surface fragmented metal usually less than .0001 inch in depth. The conception of superfinish and the designing and building of superfinishing machinery was accomplished in the plants of the Chrysler Corporation.

The author of this book is Director of Production Research for the Chrysler Corporation. He states that because there was no book devoted to the many aspects and applications of the finish of metallic surfaces, he has endeavored to develop his theme from elementary principles in order clearly to present the most advanced technical information. Accordingly, the book starts with the reasons for a surface finish, the measuring of such finishes, the tools and machines used. Every effort is made to give a thorough understanding of machining methods in sufficient detail before the superfinishing method is introduced. This subject covers considerable space and is presented in logical progression, giving the process, the technique, and results of both external surfaces and internal diameters. By discussing in detail the processing of cylinder bores in automotive engines, the entire field of bore work is included.

The relation of lubrication to surface finish is another division of the book. Here there are simple explanations of the theory of lubrication as it pertains to the theme of this book: finer surface finishes as exemplified by superfinish. There are also special topics of material and design of bearings, manufacturing and engineering advantages of superfinishing, and superfinishing machines.

The book is replete with illustrations which add tremendously to its value. Written in readily understandable language and impressive style, it is a helpful and informative means to the production of better work by the workman whether he be mechanic, technician, engineer or executive.

R. H. OPPERMANN.

ENGINEERING SURVEYS, by Harry Rubey, George Edward Lommel, and Marion Wesley Todd. Revised Edition, 141 pages, illustrations, tables, 13 × 20 cms. New York, The Macmillan Company, 1940. Price $3.50.

Surveying has been the basis of many enviable careers. A knowledge and practice of it brings forth and impresses many important attributes which are invaluable in the engineering and business world. The subject has, together with all branches of engineering, developed into a wide field, from the simple surveys of land boundaries to the extensive and difficult surveys incident to great construction projects such as a railway or an aqueduct. The simple surveys are distinguished, in this book, from the difficult surveys by naming the latter "engineering surveys" although the book covers fundamentals and gives principles from the beginning.

It opens with a discussion of the measurement of distances and the technique of keeping field notes. Descriptive matter on compass surveying, leveling, the use of the transit, adjustment and care of instruments, observations for meridian, stadia surveying, topography, triangulation and land surveys are given. Of the special branches of surveys, there is given a rather complete treatment of the survey of routes and areas, and city surveys. A very informative and helpful chapter is that devoted to the methods and procedures in the survey office, and another on the organization of surveys. The same can be said with regard to the mathematical treatment involving the computation of traverses, latitudes and departures, coordinates and areas.

The very nature of the subject requires a text to follow actual practice very closely. That is the outstanding feature of this book. Theory and practice are so close that the book may in a sense be termed a work book. Certainly the subject is well presented from the standpoint of the teacher as well as the student.

R. H. OPPERMANN.

PRINCIPLES OF DIRECT-CURRENT MACHINES, by Alexander S. Langsdorf. Fifth Edition, 746 pages, illustrations, 16 × 24 cms. New York, McGraw-Hill Book Company, Inc., 1940. Price $5.50.

The first edition of this book was published in 1915. Since that time it has been given much use. Indeed, it would be interesting to know the number of engineers to whom this was a valuable text. Three more editions have appeared since then, and now this is the fifth. The author states that the distinctive difference between this edition and the four which preceded it is that it includes a more extensive treatment of the general principles of electricity and magnetism than was possible in the single introductory chapter previously allotted to basic theory. This is a move in recognition of and toward the need for a text to meet the requirements of a changed arrangement in presenting such a course. As it stands now, there is a sufficiency of introductory matter in the beginning. This includes a historical approach to the steady flow of current in conducting circuits, and magnetism. Some one hundred pages are devoted to these subjects. Electromagnetism, electrostatics and a description of systems of electrical units cover the introductory portion of the book. With regard to the latter subject, the m.k.s. system is presented in relation to the c.g.s. electrostatic and electromagnetic systems, and to the so-called practical units.

Direct current machines proper, begins with a treatment on the dynamo, a

description of its various parts and types, the most vital of which are examined as to construction and function with relation to others and the machine as a whole. Thus, considerable effort is devoted to armature windings, the magnetizing effects of the field, and the method of predetermining a magnetization curve and magnetic leakage.

Following this a quite complete coverage is given operating characteristics of generators and auxiliary equipment including brief mention of voltage regulators. The different classes of motors is next discussed with their arrangements and connections. Much stress is laid on the theory, effects and practice of commutation and rightly so. The concluding topics are efficiency and rating, and a treatment on special machines and applications. The latter is of sufficient breadth to familiarize the student with such machines as boosters, balancers, and arc welding generators.

Of great importance to the understanding of this subject are illustrations particularly in the form of diagrams, and carefully selected and constructed problems for exercise. This book is well supplied with both. In addition, its method of presentation is one that has appeal, a cleaverly chosen road between not too much theory and not too much practice. Students who take this book seriously will have no trouble in acquiring experience in the operation of direct current machines and will have sufficient groundwork for pursuing further studies.

R. H. OPPERMANN.

THE MATHEMATICAL THEORY OF NON-UNIFORM GASES, An account of the kinetic theory of viscosity, thermal conduction, and diffusion in gases, by Sydney Chapman and T. G. Cowling. 404 pages, illustrations, 18 × 26 cms. New York, The Macmillan Company, 1939. Price $7.50.

The theory of non-uniform gases as presented here was developed not by approximate methods based on the conception of the mean free path, but by the mathematical methods originated by Maxwell and Boltzmann. The general solution of these fundamental equations was first given by Chapman in 1916 in a published generalization of the work of his first paper of 1912 in which the incorrect assumption as to the form of the velocity-distribution function was eliminated. In 1917 Enskog published his Upsala Dissertation, in which he perfected the determination of the velocity-distribution function from Boltzmann's equation. He derived general formula for the viscosity, conduction, and diffusion in simple and mixed gases, and also determined the pressure-tensor to a third approximation. The method and the details of the calculations were different from those in Chapman's paper, but the two methods give precisely the same results. Enskog was unaware of Chapman's paper of 1916 but later he took the opportunity to compare his results with those of Chapman's. This revealed a few algebraic and arithmetical errors which affected some of Chapman's formulae for the coefficients for a mixture. Since then contributions were made to the work.

In this book an account is given using the methods originated by Enskog but with some minor differences. It is attempted to expound the theory more simply than was done by Enskog especially where the argument is sometimes difficult to follow. After this there is described more recent work, on dense gases, the quantum theory and the transport phenomena, and on the theory of

conduction and diffusion in ionized gases, in the presence of electric and magnetic fields. The method of integration used in this book differs from that used by Enskog which was based on earlier work by Maxwell. For its historical interest, Enskog's method is briefly outlined in Appendix A. The general Maxwell-Boltzmann distribution velocities comprise Appendix B.

Mathematicians, physicists, and laboratory workers who are qualified will find in this book a very interesting presentation and contribution to the subject.

R. H. OPPERMANN.

GEOMAGNETISM, by Sydney Chapman and Julius Bartels. Volume I, Geomagnetic and Related Phenomena. Volume II, Analysis and Physical Interpretation of the Phenomena. 2 volumes, 1049 pages, plates, illustrations, 17 × 25 cms. New York, Oxford University Press, 1940. Price $18.00.

The many ever-day practical activities of man have brought forth a science of a distinctive character, which heretofore although existent, did not play so important a role. Standing between the science of solar physics and the more local terrestrial science of meteorology on the one hand, and the universal science of physics on the other, the science of geomagnetism is today linked with affairs such as navigation by sea and air, surveying in mines and on the surface, prospecting for minerals and oil, and communication by telegraph and radio. The authors of these books have intended them to meet a need for a comprehensive treatise on the subject. They state that recent years have seen the publication of several excellent encyclopaedia and handbook articles on the subject, an important collective work, and a few brief monographs but nothing like what is here attempted. Also there have been a large number of articles in publications in a wide field which have contributed to the subject and which, of necessity, must be assembled to enhance their value to the subject as a whole.

Volume I contains part 1 of the work. It consists of 542 pages of test on the observed phenomena of geomagnetism. Starting with a brief description of the principles of electromagnetism, there are descriptions of data other than, but closely concerned with, those of geomagnetism, namely solar and lunar data, earth currents, aurorae, and the upper atmosphere including some theoretical topics as well as a description of observed phenomena. With regard to strictly geomagnetic matters the progression is, first, the principles and methods of measurement, including an account of international co-operation in observing the earth's field—a matter of great importance in this as in other branches of geophysics, then a discussion of the main magnetic field, its secular variation, and the local anomalies which are of geological interest and of great importance in magnetic prospecting. The remainder of part 1 is concerned with the transient magnetic variations, periodic and irregular. A general review of these is given, as the three main types of transient variation are so closely interwoven in the data that it is scarcely possible to describe any one in detail without at least briefly describing the others. The two main periodic magnetic variations, which are daily, and due to the sun and moon respectively, are taken up separately. There are separate divisions of the book devoted to the various aspects of irregular variations, or disturbance of the geomagnetic field; the morphology or geographical distribution and time variation, of the main type of magnetic disturbances, which in their more extreme forms are called magnetic storms; minor types of disturbance;

various statistical features and solar relationships of magnetic disturbance; and the notable 27 day recurrence tendency due to the rotation of the sun, and the consequent changes of presentation of disturbed solar regions towards the earth.

Volume II contains part 2 and part 3 of the work. This covers 394 pages. In addition there is an extensive bibliography ingeniously arranged and classified to facilitate quick reference, a number of valuable tables, an index of authors referring to the bibliography as well as to the text, and a comprehensive subject index. Part 2 indicates how the great array of data described in part 1 are analyzed and synthesized. This opens with a treatment on harmonic analysis which discusses not only the ordinary processes but also indicates the statistical basis for the treatment of periodicities in geomagnetism. Such conceptions as conservation, the harmonic dial, the random walk, persistence and quasi-persistence, are described and illustrated by means of geomagnetic and solar data, in relation to sunspot, annual and other periods and the 27 day recurrence-tendency. This discussion is continued by dealing with the variability of solar and lunar daily variations through the use of "clouds of points" in harmonic dials. Another mathematical aspect is introduced by the spherical form of the earth and in this respect there is a description of spherical functions, in their dual cpacity as functions suitable for the mathematical expression of arbitrary distributions given on the surface of a sphere, and as appropriate solutions of Laplace's equation, allowing the separation of the earth's magnetic field into parts caused within and outside the earth's surface. These general theorems are applied to the main geomagnetic field and to the solar and lunar daily variations.

In part 3 there are discussed the physical theories which attempt to explain the various geomagnetic phenomena described in part 1 and analyzed in various ways in part 2. Here the theories of the main field and its secular variation are examined as well as the mathematical theory of current-induction by varying magnetic fields in regions bounded by concentric spheres, theories of the solar and lunar daily magnetic variations, corpuscular emissions from the sun and geomagnetic disturbance, and theories of magnetic storms and aurorae. With regard to part 3, the authors state that though real progress has been made, some of the chief problems remain unsolved and that as yet it is not easy to see whether the main advances will come from developments in atomic physics, solar physics, or radio physics.

The volumes are well supplied with illustrations—photographs, maps, drawings, etc. which are so necessary to a work of this kind. The purpose of the work has certainly been attained. It is an exhaustive, expertly prepared, comprehensive treatise on the subject—a great contribution that will go far toward progress.

R. H. OPPERMANN.

PUBLICATIONS RECEIVED.

The Social Relations of Science, by J. G. Crowther. 665 pages, 15 × 22 cms. New York, The Macmillan Company, 1941. Price $3.50.

Storage Batteries, by George Wood Vinal. Third Edition, 464 pages, illustrations, 16 × 24 cms. New York, John Wiley & Sons, Inc., 1940. Price $5.00.

National Research Council, American Geophysical Union, Transactions of 1940. Four Parts, 1146 pages, illustrations, 17 × 25 cms. Washington, The National Academy of Sciences, 1940.

United States Department of the Interior, Bureau of Mines. Minerals Yearbook, 1940. 1514 pages, 16 × 24 cms. Washington, Superintendent of Documents, 1940. Price $2.00.

Bell Telephone System, Monographs: B-1249, Temperature Effects in Secondary Emission, by D. E. Wooldridge. 13 pages, illustrations. B-1250, X-Ray Examination of Polyisobutylene, by C. S. Fuller, C. J. Frosch and N. R. Pape. 22 pages, illustrations. B-1251, The Subjective Sharpness of Simulated Television Images, by Millard W. Baldwin, Jr. 24 pages, illustrations. B-1254, The Carrier Nature of Speech, by Homer Dudley. 21 pages, illustrations. B-1255, Radio Extension Links to the Telephone System, by R. A. Heising. 36 pages, illustrations. B-1259, Ultra-Short-Wave Transmission over a 39-Mile "Optical" Path, by C. R. Englund, A. B. Crawford and W. W. Mumford. 24 pages, illustrations. 6 pamphlets, 15 × 24 cms. New York, Bell Laboratories, 1940.

CURRENT TOPICS.

Strength From Ceres.—(*Industrial Bulletin of Arthur D. Little, Inc.*, No. 163.) Current scientific overhauling of the diet has been advanced significantly by development of a "synthetic" food designed to bring even the poorest diet up to standard at low cost. Though composed predominantly of natural materials, this new food, developed by Professor Robert S. Harris and associates at the Massachusetts Institute of Technology nutritional laboratories, is synthetic in that it is compounded of several basic foods carefully selected to combine cheaply practically all nutritive elements. The food was designed primarily with an eye to economics. Intake of the different nutritive elements by the lowest income section of the population, a group very poorly fed, was first compiled and then subtracted from the optimum requirements in order to determine the deficiencies commonly encountered. Cereals, the cheapest foods, were then chosen to form the basis of the mixture. A single cereal will not support life, since its proteins lack one or more essential amino acids. However, two or three different cereals can be blended together so that one supplies deficiencies of the other. Thus by properly blending wheat and soya bean meal or oats, corn, wheat and soya bean meal a protein mixture as good as that in milk or eggs is obtained. Each of the components supplies some vitamins and minerals and remaining gaps are filled by pure mineral salts and vitamin concentrates or synthetics. Skim milk powder, a low cost by-product, can provide protein, minerals and some vitamins. The mixture lacks only Vitamin C. The resultant mixture, in flake form, is quite palatable and can be eaten dry or with milk, if desired. The daily bulk is about that of an ordinary serving of dry cereal. Twenty grams, two-thirds of an ounce, of the mixture daily, together with an additional food source to supply Vitamin C, will keep a person in good nutritional condition. Calories for energy and bulk to satisfy hunger are not provided, but these are customarily adequately available in even the poorest American diets. Thus the mixture satisfies a hidden hunger, which, unsatiated, leads to the diseases of malnutrition. Manufacturing cost of the food for one person is estimated at $1.80 per year.

R. H. O.